ANNUAL REVIEWS

Annual Review of Biomedical Engineering

Engineering Vascularized Organoid-on-a-Chip Models

Venktesh S. Shirure,[1] Christopher C.W. Hughes,[2] and Steven C. George[1]

[1]Department of Biomedical Engineering, University of California, Davis, California 95616, USA; email: scgeorge@ucdavis.edu

[2]Department of Molecular Biology and Biochemistry, University of California, Irvine, California 92697, USA

Annu. Rev. Biomed. Eng. 2021. 23:141–67

First published as a Review in Advance on March 23, 2021

The *Annual Review of Biomedical Engineering* is online at bioeng.annualreviews.org

https://doi.org/10.1146/annurev-bioeng-090120-094330

Keywords

vasculogenesis, angiogenesis, self-assembled vasculature, microphysiological systems, organ-on-a-chip, tumor-on-a-chip

Abstract

Recreating human organ–level function in vitro is a rapidly evolving field that integrates tissue engineering, stem cell biology, and microfluidic technology to produce 3D organoids. A critical component of all organs is the vasculature. Herein, we discuss general strategies to create vascularized organoids, including common source materials, and survey previous work using vascularized organoids to recreate specific organ functions and simulate tumor progression. Vascularization is not only an essential component of individual organ function but also responsible for coupling the fate of all organs and their functions. While some success in coupling two or more organs together on a single platform has been demonstrated, we argue that the future of vascularized organoid technology lies in creating organoid systems complete with tissue-specific microvasculature and in coupling multiple organs through a dynamic vascular network to create systems that can respond to changing physiological conditions.

Contents

INTRODUCTION

2D cell culture, rodents, and nonhuman primates are the conventional tools used to study human biology. While 2D models are simple (**Figure 1**), the essential premise (i.e., cell growth on plastic in nutrient baths) cannot capture the vast majority of complex cellular interactions that produce overall tissue and organ function and response to pharmaceuticals. In contrast, animal models can mimic integrated 3D functions of the body but can present severe limitations even beyond the ethical issues, including poor concordance with human biology in areas such as cardiac function, liver metabolism, and immune function. For example, patient-derived xenograft models place human cancer cells in an immune-compromised mouse to mimic tumor progression, but this approach eliminates the critical adaptive immune response to cancer present in vivo. These considerations, along with technological advances in microfabrication and stem cell biology, have spurred the creation of new model systems—dubbed organ-on-a-chip or tissue chips—that capture the multicellular, 3D nature of in vivo human tissues. In aggregate, these platforms are referred to as microphysiological systems (MPSs).

Spheroids are generally defined as single-cell 3D aggregates, whereas organoids are generally defined as 3D multicellular aggregates (**Figure 1**) that mimic one or more essential functions of an organ. Organoids are generally derived either from primary human tissues or from human pluripotent stem cells (hPSCs) (1). Organoids can be grown from either of the two main types of stem cells: (*a*) pluripotent stem cells, both embryonic stem (ES) cells and induced pluripotent stem (iPS) cells, and (*b*) organ-specific multipotent adult stem cells (1). Specialized media formulations and differentiation protocols have been developed to maintain and proliferate these organoid cultures. In the last decade, organoids have been used to model the functions of many human organs,

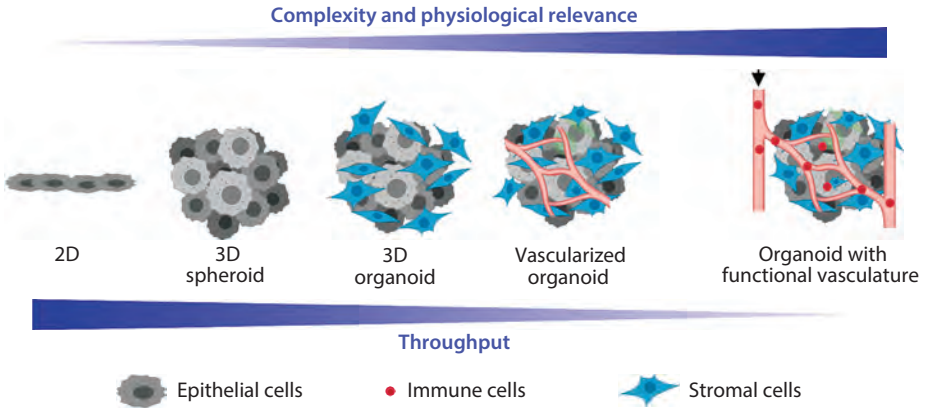

Figure 1

In vitro model systems are lower throughput but are more physiologically relevant as they increase in complexity. (*Left* to *right*) 2D monolayer culture is inexpensive and high throughput. Spheroids provide homogeneous 3D culture. Organoids are composed of different cell types that facilitate heterotypic cell–cell interactions (e.g., epithelial and stromal cells). Vascularized organoids add endothelial cells. Organoids with a perfused microvasculature allow transport of cells (e.g., immune cells) and nutrients by convection at physiological perfusion rates. Figure created with BioRender.com.

including the gut, liver, brain, bone marrow, heart, kidney, eye, lung, and microcirculation, and many different cancers. These organoids recapitulate complex 3D organ-specific structure and function, can include a vascular supply, and provide the basis for the next generation of human-specific model systems. While vascularized organoids are generally lower throughput than 2D culture and simple organoids, recent platforms have demonstrated methods to enhance throughput (2).

In parallel, researchers have leveraged the principles of the electronic chip industry's microfabrication protocols to create tissue chips. Tissue chips integrate microfluidic channels and compartments on a single platform to deliver nutrients to and remove waste from cells and organoids. Relative to traditional tissue culture wells and plates, tissue chips provide a far more dynamic and flexible environment to mimic a greater range of human biology, including 3D, multicellular tissue function and the ability to couple multiple organoids (e.g., gut and liver) in series or in parallel (3)—hence adoption of the MPS terminology. Finally, tissue chips are generally made of optically clear materials such as polydimethylsiloxane (PDMS) and therefore enable excellent 3D visualization of dynamic events with high spatiotemporal resolution.

Oxygen can freely diffuse in tissue microenvironments but is consumed by metabolically active cells. This process creates a diffusion limit in vivo, generally considered to be 100–200 μm (4). To form larger and more complex tissues, biology has overcome this diffusion limit by using a network of microvessels (capillaries) to deliver nutrients and remove waste by convection. Not surprisingly, most cells in the body are no more than 100–200 μm from a capillary. Organoids can range in diameter from 50 to 1,000 μm, but both organoid growth and function are compromised when organoid size exceeds the diffusion limit of small molecules (including oxygen). Additionally, cross talk between epithelial cells and vascular cells is critical for the appropriate growth, structure, and function of both epithelial structures and the vasculature during organ development (5). As such, integrating a perfused vascular network into organoids [i.e., vascularized organoids (**Figure 1**)] is essential to recapitulate both normal organ growth and function and to advance this important new field. Furthermore, the vasculature transports cells and signaling

molecules between organs. Thus, coupling vascularized organoids representing different organs in vitro would generate a more comprehensive platform for basic research and drug discovery. Herein, we review the fundamental strategies and successes in creating vascularized organoid-on-a-chip platforms and provide a future perspective for engineering coupled organoid culture systems. The review is organized into four major sections: (*a*) an overview of the main strategies to create in vitro vascularized organoids, (*b*) specific components needed to create self-assembled vascular networks, (*c*) specific examples of organs in which some success in vascularization has been demonstrated, and (*d*) vascularization of tumor organoids.

IN VITRO VASCULARIZATION STRATEGIES

Early 3D in vitro systems of microvessels used either a single suspension of endothelial cells (ECs) or EC-coated microbeads embedded into extracellular matrix (ECM) gels such as collagen, fibrin, or Matrigel (6, 7). These approaches yielded microvessels with lumens and were useful models of vasculogenesis and angiogenesis. However, the vessels had limited stability over time, and the model system was not conducive for perfusion through the vascular lumen or for delivery of nutrients to and removal of waste from the surrounding tissue. The emergence of microfabrication and microfluidics for biological applications led to many innovative approaches to create perfused microvascular vessels and networks of vessels (**Figure 1**). Microfluidics-based techniques to create perfusable vascular networks can be broadly categorized into two major areas: (*a*) vascular patterning (coating a patterned network of microfluidic channels with ECs) and (*b*) self-assembly (stimulating a microvessel network to self-organize through either angiogenesis or vasculogenesis and achieving a stable anastomosis with adjacent microfluidic channels).

Vascular Patterning

A general approach for patterning a vascular network is to create a network of hollow microconduits using 3D printing, soft lithography, or a combination of microfabrication techniques (8–13). ECs are then coated in a monolayer onto the surface of the conduit to create an endothelial tube. Early attempts to utilize this general strategy created the conduit by using needle etching into soft biomaterials such as collagen (8) (**Figure 2*a***). Vessels created this way remain stable and functional for 2–3 weeks and demonstrate some potential advantages, including angiogenesis into the surrounding soft biomaterial. Disadvantages include the technical challenge of manually placing and removing the needle in collagen gel, which limits throughput, and the "network" being limited to a single straight tube. Later techniques circumvented some of these challenges by using soft lithography, in which an interconnecting network of channels in a transparent polymer such as PDMS is created by casting the polymer over an SU-8 master mold. ECs are then introduced into the microfluidic lines to coat the surface (**Figure 2*b*,*c***). This approach has the distinct advantage of being highly reproducible and creates a network of EC-lined channels with prescribed dimensions that can precisely mimic in vivo vascular patterning. However, the ECs cannot penetrate the surrounding polymer, which is metabolically inert; thus, the network is not dynamic and cannot adapt to meet the changing metabolic needs of the surrounding matrix (9, 10). Additionally, the network of channels is limited to a single plane, so true 3D networks are not possible. A third major disadvantage is that the cross section of the microvessels (9–11) is generally a square or a rectangle rather than a circle. Such nonphysiological geometries discourage a continuous endothelial monolayer, as ECs tend to avoid sharp geometrical transitions, and create in vitro artifacts; for instance, rectangular microvessels sprout mainly at the corners of the vessel (14). Finally, the shear stress on the ECs at different channel positions is more variable in a square or a rectangular shape than

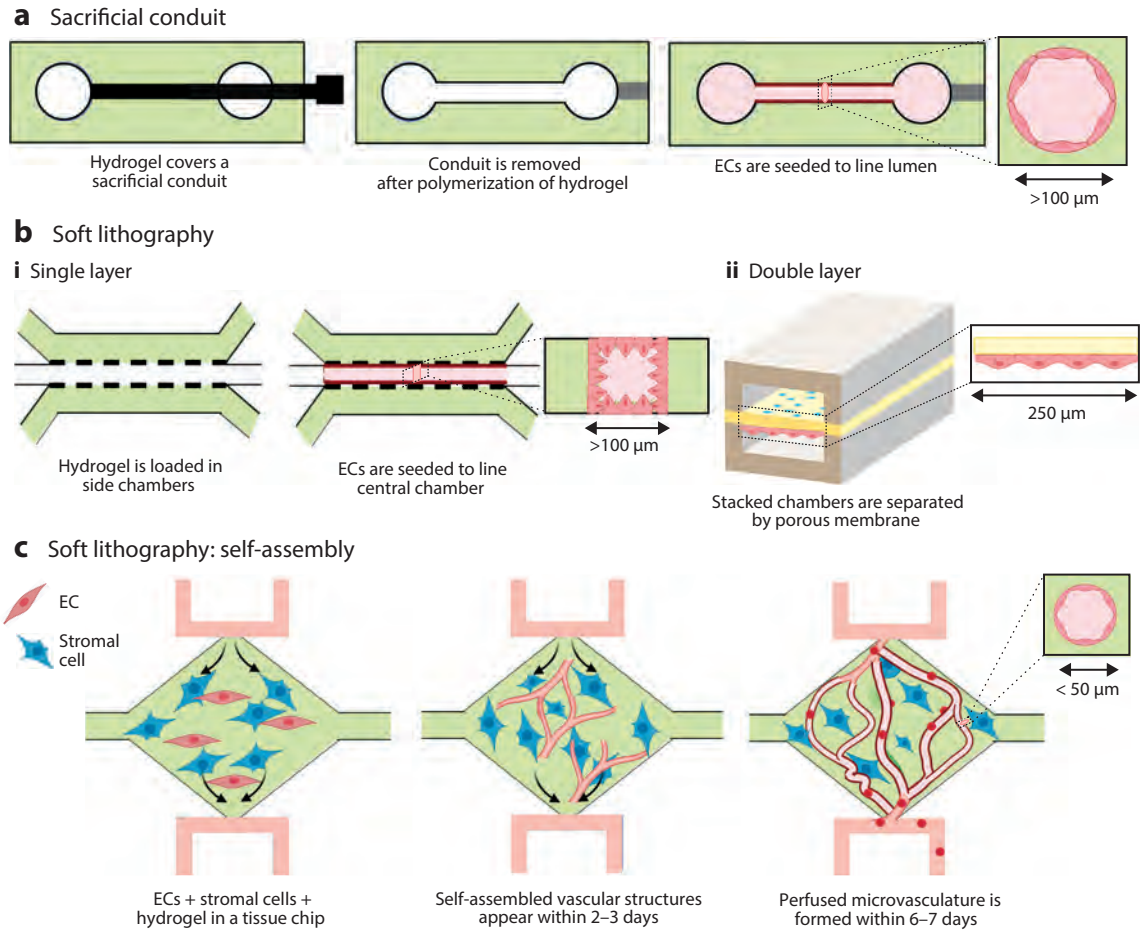

Figure 2

Vascularization strategies. (*a*) A single channel mimicking a vessel can be created by placing a hydrogel around a sacrificial conduit (e.g., needle etching), followed by coating of the microconduit with endothelial cells (ECs). A cross section of the vessel is shown at the far right of panel *a*. (*b*) Hollow EC-coated conduits can also be made using a microporous membrane to separate (*i*) matrix-filled chambers in a single-layer design or (*ii*) two adjacent fluid-filled chambers in a double-layer device. (*c*) Alternatively, ECs (*red*) and stromal cells (*blue*) can be mixed with a hydrogel and seeded in a device created using soft lithography under controlled interstitial flow (*black arrows*) and growth conditions to allow a vascular network to self-assemble. Vascular structures appear within 2–3 days, which then connect to form an interconnected, branched, and perfused microvasculature. A cross section of the vessel is shown at the far right of panel *c*. Figure created with BioRender.com.

in a native circular shape, and such variability impacts cell physiology and inflammatory response (15, 16).

An alternative approach to pattern a microvessel network utilizes a PDMS stamp to reverse cast a conduit in a collagen gel by using injection molding. This technique can be used to create multiple parallel microvessels in collagen (11). In an effort to counter the sharp corners present in square and rectangular channels, viscous fingerprinting has been employed. In this approach, a less viscous fluid is pumped through a hydrogel while its polymerization is still incomplete, creating a hollow cylindrical conduit in the hydrogel after polymerization (12). A major advance in patterning vessel networks is bioprinting a sacrificial carbohydrate lattice (13). A soft biomaterial

such as collagen or fibrin can then be cast around or over the lattice and allowed to polymerize, after which the sacrificial lattice is dissolved (generally by exposing the 3D construct to water). ECs can then be introduced to coat the channels. This technique not only produces circular channels but also creates a true 3D network of channels, allowing for vessel sprouting or angiogenesis into the surrounding soft biomaterial. Additional details on patterning techniques to create vessel networks have been presented in a series of reviews (17–19).

While these methods provide consistent density and geometry of vessels and a predictable intraluminal flow, there is no in vivo biological analog for these vascularization methods. The microvessels formed using these techniques are generally much larger in diameter (>100 μm) than in vivo capillaries (<20 μm) and result in vessel densities (<10 per mm^2) that are an order of magnitude smaller than those present in vivo (20, 21). Finally, the networks are inspired by engineering technology; that is, the dimensions and branching nature are prescribed by the engineering technology and are thus created using an engineering-directed approach. An alternative approach is biology directed and harnesses the intrinsic forces of biology to generate the vessel network.

Self-Assembly

In vivo tissue is vascularized through angiogenesis or vasculogenesis. In angiogenesis, new vessels sprout from an existing vessel, and in vasculogenesis the ECs assemble de novo into a network of vessels. Of note, vessels formed by vasculogenesis can subsequently undergo angiogenesis. Several labs, including our own, have developed protocols to create in vitro microvascular networks that mimic developmental vascularization. We refer to this as a biology-directed approach (22–29) (**Figure 2**), in contrast to the engineering-directed approaches described above. The underlying premise of these protocols is to place ECs and stromal cells together in a hydrogel (collagen, fibrin, or Matrigel) in what is initially a random spatial distribution. Over the ensuing 3–7 days, the ECs migrate, make contact, align, form lumens, and generate a complete perfusable network; in other words, the intrinsic biological programming present in the ECs and stromal cells allows the vessel network to self-assemble (22–26). An alternative approach is to coat neighboring porous microfluidic channels with ECs and to allow the ECs to sprout, by angiogenesis, into the adjacent matrix that separates the channels (27–29). The sprouting vessels from each channel will anastomose to create a perfusable vascular network.

By using either of these self-assembly techniques, stable perfusable microvessel networks have been achieved, with microvessel diameters generally in the range of 15–50 μm. The vessel geometry (diameter and length), density, branching, perfusion, stability, and permeability depend on the biophysical (e.g., interstitial flow, intraluminal flow, matrix stiffness) and biochemical [e.g., vascular endothelial growth factor (VEGF)] cues provided to the ECs from the surrounding matrix and stromal cells (29–31). This approach engages the complex interplay of cells, ECM, and physical forces to dictate the characteristics of the network. Since the initial description of this technique, there has been a significant advancement in our understanding of both the biology and the necessary engineering.

COMPONENTS OF SELF-ASSEMBLED MICROVASCULATURE

Endothelial Cells

Protocols have been established to utilize human umbilical vein ECs (HUVECs) and endothelial colony–forming cell ECs (ECFC-ECs) from human umbilical cord and cord blood, respectively, to create in vivo and in vitro vascular networks (20, 32, 33). The latter are derived in culture from endothelial progenitor cells (EPCs), which are found in embryonic tissues and display true

angioblastic potential, high plasticity, and high proliferation capacity. Compared to HUVECs, cord blood–derived ECFC-ECs have greater vasculogenic potential and ability to form perfused networks in vivo (32). EPCs from adult blood, while much lower in concentration than in cord blood, have also been used to create microvasculature in vivo (20, 33). However, these microvessels are less stable than vessel networks formed using embryonic tissue–derived ECFC-ECs (20, 33).

hPSC-derived ECs (hPSC-ECs) provide a potentially inexhaustible supply of ECs from the same donor, as well as several other advantages. First, concerns over donor-to-donor variability in primary cells are ameliorated. Second, the hPSC cell line can be genetically modified to create stable subclones by using advanced gene editing technologies such as clustered, regularly interspaced, short palindromic repeats (CRISPR)-Cas9. The subclones can serve as powerful biological tools for mechanistic studies (34). Finally, the technology has the potential to allow modeling of patient-specific tissues in vitro, and such tissues can be used in precision medicine applications (35). Numerous protocols have been developed to create hPSC-ECs, but the general approach utilizes GSK3 inhibition and BMP4 treatment to convert hPSCs into mesodermal cells, followed by exposure to VEGF-A or platelet-derived growth factor BB to produce functional ECs or smooth muscle cells (36). We have demonstrated the feasibility of creating perfused microvascular networks-on-a-chip by using iPS cell–derived ECs (37). In addition, other groups have demonstrated the use of hPSC-ECs to create microvasculature that is perfusable in vivo (35, 38).

Microvascular ECs collected from adult organs display differences in both structural attributes and molecular expression profiles (39–41). In one study, ECs of four major human organs—the heart, lung, liver, and kidneys—were isolated from fetal tissues. The ECs demonstrated distinct expression patterns of gene clusters, barrier properties, angiogenic potential, and metabolism (39). Although organ-specific microvascular ECs can be used for vascularization for some organs [e.g., dermal ECs (42)], this source of ECs, in general, has very limited vasculogenic potential (even lower than do adult peripheral blood ECFC-ECs) (33). It is therefore of interest to determine whether ECs differentiated from EPCs, if given appropriate cues, can exhibit organ-specific features. Notably, ECs demonstrate phenotypic plasticity in molecular expression when isolated and cultured in vitro (39). In line with this finding, cord blood–derived ECFC-ECs change expression of several hundred genes in response to altered microenvironments (43).

Stromal Cells

ECFC-ECs embedded in a hydrogel by themselves form poor microvasculature with incomplete or no luminal structures (30, 31, 44). The incorporation of stromal cells, such as fibroblasts, in the coculture facilitates the formation of microvessels with stable lumens (44). The separation distance of stromal cells from ECs is also important; while physical contact is not required, if the stromal population is too far away, stable vessels will not form (44). Stromal cell–derived angiopoietin-1, angiogenin, hepatocyte growth factor, transforming growth factor-α, and tumor necrosis factor (TNF) have been identified to drive EC sprouting (30). Five additional genes expressed in fibroblasts—the genes encoding collagen I, procollagen C endopeptidase enhancer 1, SPARC (secreted protein acidic and rich in cysteine), the transforming growth factor β (TGFβ)-induced protein ig-h3, and insulin growth factor–binding protein 7—have been demonstrated to be crucial for lumen formation (31). Stromal cells also impact the ECM through the expression and secretion of matrix metalloproteinases, tissue inhibitors of metalloproteinases, fibronectin, and collagen to facilitate lumen formation (30, 31, 45). Moreover, stromal cells can impart micromechanical forces to facilitate microvasculature formation and angiogenesis (46). The support of stromal cells is particularly important in early stages of morphogenesis, and their selective depletion in later stages does not appear to affect the developed microvasculature (28).

Stromal cells from a wide range of sources—including lung (24, 26), skin (42), bone marrow (25) [including mesenchymal stem cells (MSCs) (47)], and cancer-associated fibroblasts (CAFs) (46)—have been demonstrated to support stable microvessel network formation. More recently, protocols have been established to differentiate stromal cells from hPSCs (38, 48); these stromal cells also support self-assembly or vasculogenesis of ECs into stable microvascular networks (38, 48).

Interstitial Flow

Tissues developing in vivo experience interstitial flow in the range of 0.1–10 μm/s as fluid leaks from the capillaries and is reabsorbed by both blood and lymphatic capillaries (49). Interstitial flow through the tissue aids in the transport and distribution of nutrients and growth factors, as well as in the removal of waste from the tissue. Interstitial flow influences the development of capillaries and remodeling of the ECM by stromal cells (49, 50). We observed that interstitial flow in the physiological range (1.7–10 μm/s) facilitates vascular network formation and enhances both vessel length and branching (51). Interstitial flow also exerts fluid forces on ECs and provides directional cues for budding vessels. Both (*a*) the shear forces exerted by interstitial flow passing through the vascular wall [intercellular or transmural flow (52)] and around the vessel (50) and (*b*) the pressure forces (53) exerted by the flow facilitate sprouting of vessels in the upstream direction. The sensing of the directional cues in this process is attributed to integrins (50) and associated focal adhesion proteins (53).

Because interstitial flow imparts guidance cues to sprouting microvessels, it can be specifically leveraged to design and create perfused microvascular networks in a microfluidic device (23, 24, 29). As described above in the section titled Self-Assembly, a perfused microvascular network can be formed by distributing ECs and stromal cells in a hydrogel. A particular challenge in this method is that the microvessels must connect (anastomose) to an adjacent microfluidic line to become perfused but must also receive nutrients during development. We demonstrated that interstitial flow can be used to accomplish both needs. Interstitial flow is used (*a*) first to deliver nutrients and remove waste from the developing network and (*b*) then to guide vessels to connect to the microfluidic pore connecting the tissue chamber and the microfluidic line (23, 24, 29).

Extracellular Matrix

A critical component in the design of microvascular networks is the hydrogel or ECM. The properties of the hydrogel that impact the microvascular network include density, degradability, viscoelastic properties, and integrin binding sites. For example, high fiber density provides good structural support but can retard the transport of paracrine morphogens and limit capillary morphogenesis (54, 55). Stromal cells can remodel the hydrogel by secreting metalloproteinases and depositing new ECM (30, 31, 45). The remodeling process can improve transport of paracrine morphogens, thus enhancing capillary morphogenesis (47). Soft matrices facilitate angiogenesis; however, stiff matrices provide strong directional cues for angiogenesis, as sprouts align along a VEGF gradient more readily in stiff than in soft ECM (55). Finally, an increased number of integrin binding sites enhances mechanotransduction and vessel stability (56).

The abundant and naturally occurring ECM proteins, including fibrin and collagen, possess optimal qualities to support microvascular networks and have been used extensively by many groups (24–26, 42, 57). The entire ECM can be harvested by tissue decellularization from normal or tumor tissue (58, 59), or individual proteins can be purified from nonhuman sources (e.g., bovine or rat tissue). These proteins possess the natural and necessary binding sites for the EC and stromal

cell to elongate, migrate, proliferate, and remodel the ECM. All of these functions are required for the self-assembly and maintenance of a stable vascular network. The primary disadvantage of these proteins is lot-to-lot variability in functional properties when they are procured from commercial sources. This hurdle can generally be overcome by the 3D vascular network itself, as the cells actively remodel the starting components of the matrix. In contrast, synthetic biodegradable polymers have also been presented; examples include hyaluronic acid–based matrix (60), methacryloyl-modified gelatin hydrogel (61), and poly[octamethylene maleate (anhydride) citrate] (62). These materials provide a high level of control over mechanical and degradative properties, but they often have low permeability for paracrine morphogens, and robust, stable vessel networks have been difficult to create and maintain. These topics are extensively covered elsewhere (e.g., 56).

ORGAN-SPECIFIC VASCULARIZED ORGANOIDS

Below we briefly describe organ-specific vascularized organoids, including bone marrow, brain, heart, pancreas, liver, intestine, kidney, and lungs. This list of organs is not meant to be exhaustive but includes major organs for which significant success or attention to vascularization has been demonstrated.

Bone Marrow

Bone marrow is a highly vascularized organ whose primary function is hematopoiesis. It can also be a site of metastasis of several types of cancers, including breast and prostate cancers. The key components of bone are MSCs, hematopoietic stem/progenitor cells (HSPCs), osteoblasts, adipocytes, fibroblasts, ECs, and mineralized bone. Since the cellular component of bone marrow in vivo is essentially a liquid, a bone marrow organoid requires a casing or container, which previous work achieved by leveraging a self-assembled vascular network in the presence of bone marrow cells (**Figure 3*a***). Initial attempts to create an in vitro 3D model of bone marrow used bone from animal models and were focused on retaining the properties of bone marrow cells in culture (63, 64). To create a human-specific model, protocols have been developed to differentiate bone marrow–derived MSCs isolated from human bone marrow aspirate into perivascular or osteogenic cell lineages (64–66). The bone marrow MSCs undergo a phenotypic transition toward perivascular cell lineages if these cells are maintained in endothelial growth medium (65). Moreover, when cocultured with HUVECs in decellularized bone scaffold and fed with specialized endothelial growth media, these bone marrow MSCs support self-assembled vascular networks (64). Alternatively, MSCs differentiate into osteogenic cells if maintained in media that contain osteogenic factors, such as dexamethasone, sodium-β-glycerophosphate, and ascorbic acid-2-phosphate (64, 66). As an alternative to invasive bone marrow aspirations, human adipose tissue–derived stem cells separated from skin can be differentiated into a bone matrix and can support a self-assembled microvessel network (61). Soft and stiff hydrogels created by using methacryloyl-modified gelatin hydrogels, instead of animal bone, can also be used to support microvasculature and osteogenesis (61). The most recent example of a vascularized in vitro model of bone marrow utilized the process of vascular patterning and seeded ECs on a channel adjacent to a stromal compartment, thereby successfully mimicking features of patient-specific bone marrow toxicity (67).

The multipotency of HSPCs is difficult to maintain in 2D in vitro culture systems. HSPCs have been demonstrated to maintain the multipotent state ($CD34^+$ $CD38^-$) if seeded with bone marrow–derived stromal cells in close proximity with a patterned EC monolayer (68). Our own group recently reported on the creation of adjacent perivascular and endosteal bone marrow niches that included perfusable self-assembled vascular networks (69). The in vitro model demonstrated

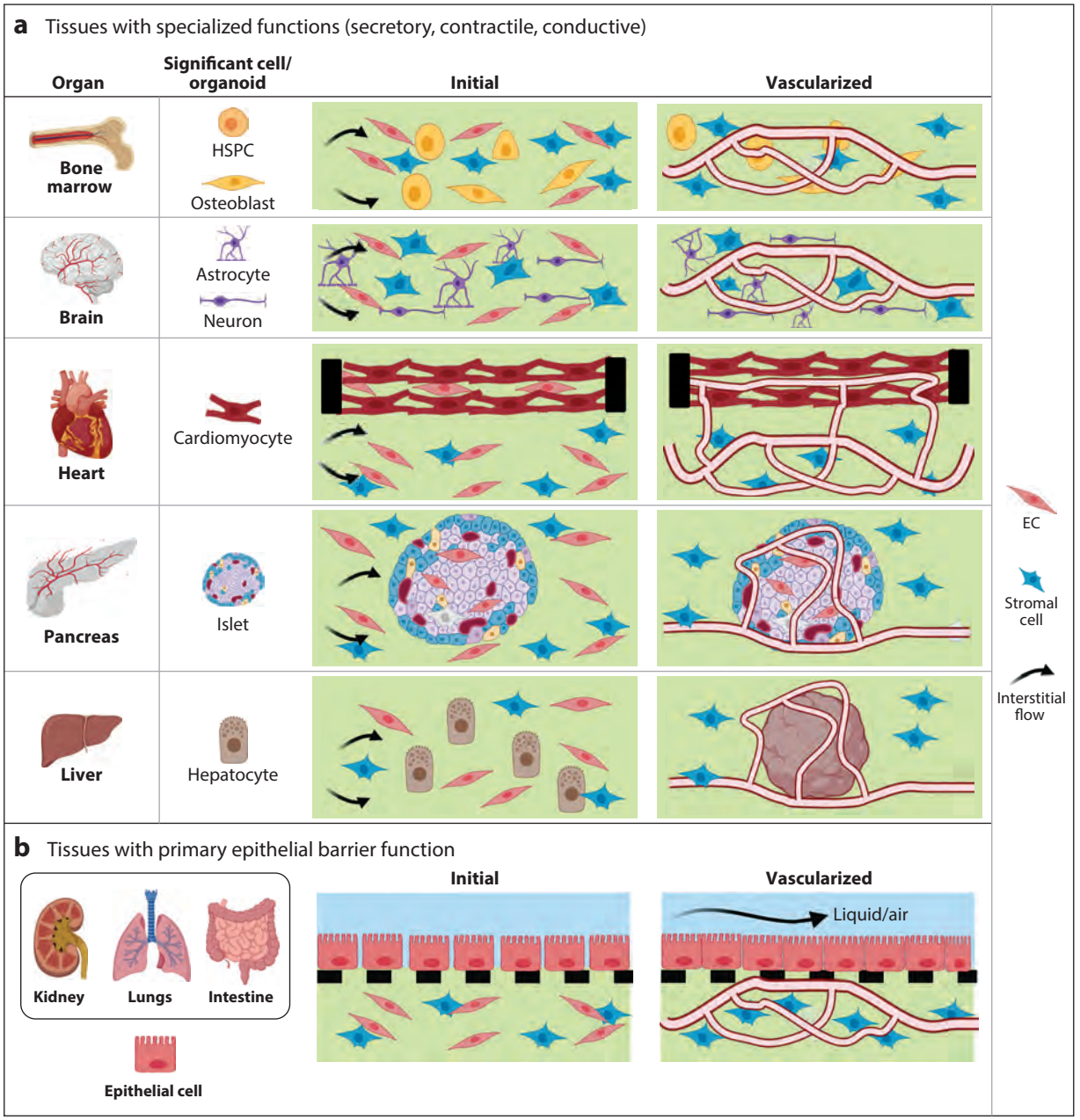

Figure 3

Strategies to create organ-specific vascularized organoid-on-a-chip systems. (*a*) Tissues with primary secretory (e.g., liver and pancreas), mechanical (e.g., heart), or specialized (e.g., brain, bone marrow) functions can be created using a range of strategies in which organ-specific cells or organoids are introduced with ECs and stromal cells and the vascular network is allowed to self-assemble. Organoid and vascular network formation is generally improved in the presence of interstitial flow. (*b*) Alternatively, tissues characterized by absorption of molecules across specialized epithelial surfaces (e.g., lung, intestine, kidney) can be created by placing the specialized epithelial cell as a monolayer over a semipermeable barrier patterned with soft lithography. Air or liquid can flow over the epithelium, and the underlying adjacent compartment can then be seeded with ECs and organ-specific stromal cells to enable self-assembly of a vascular network. Abbreviations: EC, endothelial cell; HSPC, hematopoietic stem/progenitor cell. Figure created with BioRender.com.

physiological permeability of the microvasculature, maintenance of the multipotent phenotype of HSPCs, hematopoiesis, and the egress of mature neutrophils into adjacent microfluidic lines, thereby mimicking natural functions of bone marrow (69). The vascularized bone marrow chips can qualitatively recapitulate bone formation, hematopoiesis, and cellular egress.

Brain

The brain microvasculature is unique because its transendothelial transport barrier is more selective than any other network in the body; this property is termed the blood-brain barrier (BBB). ECs, astrocytes, pericytes, and a complex ECM compose the neurovascular unit, and the cross talk between these components induces a high level of tight-junction protein expression in the EC, along with a decrease in paracellular transport as a consequence of the downregulation of plasmalemmal vesicle–associated protein (70). Several MPS models of the BBB have been developed (71–73); however, only a few have a perfused vascular network, mostly relying instead on engineered single channels (70). Transepithelial electrical resistance (TEER) of a monolayer of ECs nearly quadrupled when the monolayer was cocultured with rat primary astrocytes (74). An oscillating shear was used to achieve a peak TEER of 4,400 $\Omega \cdot cm^2$ (71), which is within the in vivo BBB range (1,500–8,000 $\Omega \cdot cm^2$) (75). Recently, iPS cell–derived ECs were cocultured with human primary brain pericytes and astrocytes to form a self-organized microvasculature in a microfluidic device. The permeability of these microvessels was 8.9×10^{-8} cm/s and 2.2×10^{-7} cm/s for 40 kDa and 10 kDa fluorescently labeled dextran, respectively; these measurements are comparable to values from in vivo rat cerebral microcirculation (76). Interestingly, the barrier properties of iPS cell–derived brain microvascular endothelial cells improve in coculture with astrocytes and neurons relative to coculture with either astrocytes or neurons alone (77), showing the importance of parenchymal cells for retention of brain-specific features of the vasculature.

Coculture of vascularized brain organoid models and neurons has been used for disease modeling, reflecting the important role that neurovascular coupling plays in the pathogenesis of neurodegenerative disorders (70). Human ES cell–derived motor neuron spheroids and iPS-ECs or HUVECs cultured in a microfluidic device create 3D, perfusable vascular networks. The microvascular networks promote synaptic connectivity, and motor neurons influence vascular network formation (57). The coculture of human ES cell–derived neural progenitor cells, ECs, MSCs, and microglia/macrophages in polyethylene glycol hydrogels is reported to generate self-assembled vascular networks and neural constructs with diverse neuronal and glial populations and microglia (78). This coculture system is reproducible and can be used as a predictive tool for neurotoxicity screening of chemical compounds (78).

A linked organ-on-a-chip model of the human neurovascular unit was recently developed and used to demonstrate metabolic coupling of the vasculature to neurons; specifically, this coupling led to increased synthesis and release of neurotransmitters, including GABA (79). Numerous neurological diseases—including Alzheimer's, Huntington's, and Parkinson's diseases and multiple sclerosis (70)—have been linked to a dysfunctional BBB, and so a vascularized brain model will undoubtedly prove invaluable in furthering understanding of these diseases.

Heart

Proper heart function depends on highly synchronized and coordinated contraction of cardiac muscle—the result of electromechanical coupling at the single-cardiomyocyte level and the tightly coupled interactions between cardiomyocytes and supporting stromal cells. Not surprisingly, the high workload of the cardiac muscle is matched by a high metabolic rate that is maintained

exclusively through oxidative phosphorylation. The resulting oxygen demand is met in vivo with an extensive vascular network in which the distance between a capillary and the nearest cardiomyocyte is as small as 1 μm (80); this network delivers oxygen by convection throughout the 3D cardiac muscle.

Development of a perfused vascularized cardiac organoid (**Figure 3*a***) is particularly challenging for several reasons. First, primary adult cardiomyocytes with a contractile phenotype are difficult to maintain in vitro and do not proliferate in culture. Second, the contractile function of cardiomyocytes creates hurdles to capturing imaging endpoints and requires additional spatial degrees of freedom in culture. Third, cardiac muscle is cell dense, with an intrinsically high metabolic rate and oxygen demand. Despite these challenges, long-term culture of contractile cardiomyocytes in a 3D environment has been demonstrated, and the use of cardiomyocytes generated from hPSCs has been extensive over the past decade (81) but has been beset with an immature phenotype. More recently, contractile conditioning of a 3D iPS cell–derived cardiac tissue construct demonstrated remarkable maturation and phenotypic features of adult cardiac tissue (82), although a vascular supply or vascular network was not demonstrated. Both adult cardiac matrix and a 3D microenvironment improve iPS cell–cardiomyocyte maturation (83), while ECs provide cardioprotective effects in vitro and ECs and cardiac fibroblasts improve proliferation rates of cardiomyocytes (84–86).

The unique features of cardiac muscle necessitate unique device designs. A coculture of (*a*) human coronary artery ECs, (*b*) cardiac fibroblasts, and (*c*) adult cardiomyocytes or iPS cell–derived cardiomyocytes in a hanging drop resulted in vascularization of the tissue (87). In another approach, cardiac cell sheets produced from coculture with ECs were triple layered to produce a 3D structure (84). Of note, the ECs in this cardiac sheet model formed lumens that were perfusable and that could anastomose with host vasculature upon implantation. To create thicker tissue, cardiomyocytes derived from iPS cells, ECs, and fibroblasts were combined to make spheroids, and the spheroids were assembled into a tubular construct by using bioprinting (88). The cardiac construct could be electrically paced at high frequencies, yet returned to baseline beat rate after stimulation ceased. Our group recently created an integrated chip of cardiac and colon cancer tissues to assess the efficacy and cardiotoxicity of chemotherapeutics. This chip integrated electrodes in the chip for stimulation of cardiomyocytes and had a patterned microvasculature to introduce drugs through the vascular mimic (89). A 3D cardiac organoid composed of cardiomyocytes, supporting stromal cells, and a perfusable microvessel network remains to be developed.

Pancreas

Pancreatic islets are the functional unit of the endocrine pancreas and are highly vascularized in vivo—they constitute only 1% of the pancreas, yet receive 15% of blood flow to the pancreas (90)—and each insulin-secreting beta cell is associated with at least one EC. As is the case in many organs, the pancreatic vasculature has a distinct phenotype; in this case, it is highly fenestrated. In addition to insulin-secreting beta cells, the islets contain alpha and delta cells, which secrete glucagon and somatostatin, respectively. Protocols to obtain these cell types from iPS cells are being developed; however, to accurately model the appropriate cell composition and functionality, cadaveric human islets are used. One study found that encapsulation of islets with collagen and HUVECs facilitated vascularization following in vivo implantation (91), and similar strategies are being pursued in vitro (**Figure 3*a***). Although isolated islets are small (<1 mm in diameter), due to their high rates of metabolism, long-term maintenance in culture is a problem. The functionality of islets can be improved somewhat by increasing the interstitial flow (92), and they are often maintained in perfusion devices, but for long-term culture of pancreatic islets, vascularization

strategies are needed. Several groups, including ours, are currently developing microfluidic-based, vascularized human islet platforms, and one of these has been published (93). However, no glucose-stimulated insulin release was demonstrated, so the functionality of these islets is yet to be demonstrated (93). Type I diabetes is an autoimmune disorder that involves the destruction of beta cells, likely by a combination of T cells and macrophages. The use of models employing perfused vasculature will be essential for the accurate reproduction of lymphocyte and monocyte/macrophage delivery to tissues.

Liver

During liver organogenesis, newly specified hepatic cells from endoderm interact with ECs and mesenchymal cells to form vascularized liver tissue (94, 95). Several groups are developing liver MPSs, although not all these groups are including vasculature, and these efforts were recently reviewed (96). A key structural feature of the liver is the organization of the vasculature; such organization allows for oxygen gradients across the lobules that generate zones of differing metabolic function. In addition, the highly fenestrated vasculature allows for high interstitial flow through the liver. These functions will ideally be incorporated into MPS models to allow for full functionality, but this goal has not been met. In the meantime, human iPS cell–derived hepatic endoderm cells (94) or human fetal liver cells (95) cocultured with HUVECs and umbilical cord–derived MSCs have been shown to form vascularized liver buds that anastomose to host vasculature in vivo (94, 95). The hydrogel used in these studies was critical for this process: Matrigel (laminin, collagen IV, and entactin) (94) or a combination of collagen I and fibronectin (95) supported optimum bud formation, but collagen I, laminin, or agarose did not. Moreover, the density of the gel is also critical; dense Matrigel did not support liver bud formation (94). In a separate study, human primary hepatocytes and normal human dermal fibroblasts were precoated with the ECM proteins fibronectin and gelatin. HUVECs mixed with these cells create lumen structures, and in studies in vivo, the vascularized tissue starts producing albumin earlier than a nonvascularized tissue or hepatocyte suspension does (97). Bioprinting has also been used to create tissues containing hepatocytes and HUVECs. Microvascular structures form but are not perfused. Despite this lack of perfusion, the combination of ECs and hepatocytes produced more albumin and urea than did hepatocytes cultured alone, suggesting a positive trophic effect of ECs (98). A liver MPS model (99) was recently coupled to several other tissue MPS systems to create an integrated systems model; however, vasculature was not incorporated (100).

Intestine

The gut includes a range of discrete anatomical regions, including the mouth, oropharynx, larynx, esophagus, stomach, small intestine, and large intestine. Smaller structures within the gut include sphincters separating the regions (e.g., lower esophageal sphincter), and there are subdivisions within the small intestine (i.e., duodenum, jejunum, and ileum) and large intestine (i.e., cecum, appendix, ascending colon, descending colon, sigmoid colon, rectum, and anal canal). These different regions have discrete functions and microbiota, all of which impact the vascular supply. Most attempts to model the primary functions of the gut have focused on the large and small intestines. The intestinal lumen is lined by epithelial cells that provide an absorptive surface for nutrients and drugs but that can also be sites of acute inflammation, cancer, and infection. The microvasculature lies just beneath the epithelium and plays a critical role in intestinal function. As such, a successful strategy to create vascularized models of the intestine has utilized a patterned organ-specific epithelium overlying a vascular network (**Figure 3*b***).

The three major cell types used to create vascularized intestinal organoids are intestine-specific epithelial cells, myofibroblasts, and ECs. Protocols have been established to derive intestinal epithelial and myofibroblast cells from both hPSCs and primary human tissue specimens (101–105). The hPSC-derived organoids self-organize into structures that include a lumen, villus-like structures, and crypt-like proliferative zones (101, 102). The organoids also consist of all the major epithelial cell types, including enterocytes, goblet cells, Paneth cells, and enteroendocrine cells. The intestinal myofibroblasts support the self-assembly of a microvascular network from HUVECs and cord blood–derived ECFC-ECs (103, 104). Although primary microvascular ECs extracted from intestine have been used to create microvessels by patterning (105), the potential of these ECs to self-assemble into a vessel network has not been shown. Not surprisingly, the microvascular networks directly impact the function of the intestinal epithelium. For instance, coculture of ECFC-ECs with patient-derived intestinal myofibroblasts and ileal epithelial cells in a microfluidic platform improved the barrier function of the intestinal epithelial cells (104). Other studies have placed endothelium-coated tubes next to intestinal epithelial cell–coated tubes separated by a flexible microporous membrane (106). These studies have recreated an impressive array of intestinal functions, including the maintenance of a bacterial colony to simulate the human microbiome (106). Finally, patient-derived organoids from the small intestine have been shown to form villi-like projections lined by epithelial cells that undergo multilineage differentiation (105).

Kidney

The key functions of the kidney include removal of waste products from the blood, especially urea (the primary nitrogenous by-product of protein metabolism), and maintenance of water balance. The kidney has an extensive vascular supply and receives approximately 20% of the cardiac output. Waste products, excess water, solutes, and drugs are removed from blood, while essential components, including glucose, proteins, and other solutes, are retained. The functional unit of the kidney is a nephron, which consists of an epithelialized lumen through which the effluent passes while the lumen constantly exchanges mass with the surrounding stroma. The distinct parts of a nephron include the glomerulus, proximal tubule, loop of Henle, and distal tubule, which provide specialized filtration of molecules. A protocol to differentiate hPSCs into kidney epithelial and parenchymal cells has been developed (107). These organoids self-assemble into lumenized structures and display epithelial markers specific for all types of nephron cells (107). A general strategy to create access to the lumen is to create patterned conduits of the epithelial cells (108) (**Figure 3*b***). Such strategies have been applied to create the proximal tubule to demonstrate reabsorption, albumin transport (109, 110), and glomerular function to demonstrate ultrafiltration (111). The human kidney microvascular ECs exhibit barrier function and have the capacity to self-assemble (112). However, their angiogenic potential is lower than that of HUVECs, and thus supplementing the media with a high concentration of VEGF (40 ng/mL) has been required for the self-assembly assays (112).

Lungs

The primary function of the lungs is respiratory gas exchange (of O_2 and CO_2). The lungs are characterized by two major regions. The first region is the delicate alveolar tissue, which is composed of grapelike clusters of small (50–100 μm in diameter) air-filled sacs termed alveoli. The alveoli are characterized by a very thin membrane (on the order of 0.5 μm) that separates the air from the blood in the pulmonary circulation and is the site of respiratory gas exchange. The alveolar membrane has an air interface; consists of type I and type II epithelial cells, ECs, and

fibroblasts; and experiences cyclical strain during breathing. The alveoli also contain leukocytes (e.g., macrophages) and have important roles in host defense. Circulation through the alveoli is derived from the right side of the heart, which represents cardiac output. The second major region of the lungs is the branching airways, which provide a conduit for air to travel from the outside environment to the alveolar region, and vice versa. The airways contain a thin layer of smooth muscle that can become overactive, leading to airway constriction—a hallmark of bronchial asthma. The airways have a separate circulation—the bronchial circulation—that is derived from the left side of the heart and serves to provide nutrients and remove waste products from the airway tissue. Similar to the intestine and kidney, an attractive approach to model the alveolar and airway regions of the lungs is a patterned epithelium overlying a self-assembled vascular network (**Figure 3*b***).

Tissue chip modeling of the lung really launched the field of tissue chip modeling with a seminal report in 2010 (10). In this model, a simple monolayer of alveolar epithelial cells and ECs was cultured on opposite sides of a porous flexible membrane to mimic the alveolar membrane. The flexible membrane was subjected to cyclical strains, recreating forces present in native tissue, and the model allowed for analysis of immune cell trafficking, disease, and drug treatments (10, 113, 114). Less work has been reported using stem cell–derived lung cells or organoids, but lung epithelial cells derived from hPSCs have been shown to express specific markers and perform certain functions, including secretion of surfactant by type II epithelial cells (115, 116). The lung epithelial cell structures in these organoids are surrounded by smooth muscle and myofibroblasts (116). The coculture of bronchial epithelial cells, lung fibroblasts, and ECs (HUVEC or lung derived) in an ECM (fibrin or Matrigel) has also been reported as a model of angiogenesis in the airways (117). In addition, the self-assembly of discrete epithelial and endothelial structures with lumens has been demonstrated (118). Furthermore, lung fibroblasts exhibit the exceptional ability to support the self-assembly of vascular networks; as such, a wide range of research groups have used these cells in multiple models (7, 24, 29, 119–121).

An ideal model of the alveolar region of the lung would recreate its spherical geometry, would include a dynamic model of the pulmonary circulation and interstitial space, and would mimic important diseases processes such as pulmonary hypertension and fibrosis. Similarly, the ideal model of the bronchial airway would include airway smooth muscle, a dynamic circulation that could undergo angiogenesis, and the airway epithelium. Our understanding of the pluripotent stem cells necessary to create these complex structures by self-assembly is still evolving. As such, an engineering approach that combines patterning techniques with the self-assembly of anatomical structures could be a productive direction to create the next generation of vascularized lung organoids.

VASCULARIZED TUMOR ORGANOIDS TO MODEL TUMOR PROGRESSION

Modeling of cancer progression and drug response has historically been dominated by 2D cell culture and mouse models. Unfortunately, 2D models are constrained by their inability to model the complex, 3D nature of the tumor microenvironment (TME). For example, most tumor cells are programmed with redundant and dynamically changing pathways that control differentiation, migration, and cellular response to exogenous factors. Furthermore, a growing body of evidence demonstrates that tumor cells display significant phenotypic plasticity in 3D cultures relative to 2D cultures (122–126). Cell–cell interactions and cytokine cross talk involving immune cells, CAFs, ECs, and tumor cells are critical for cancer growth, response to treatment, and development of drug resistance (127–129).

In contrast to 2D cell culture, animal models are outstanding at simulating the aggregate response of the tumor and host, but they have a limited ability to mimic human biology and have limited spatiotemporal resolution to probe molecular events. Modeling cancer progression and

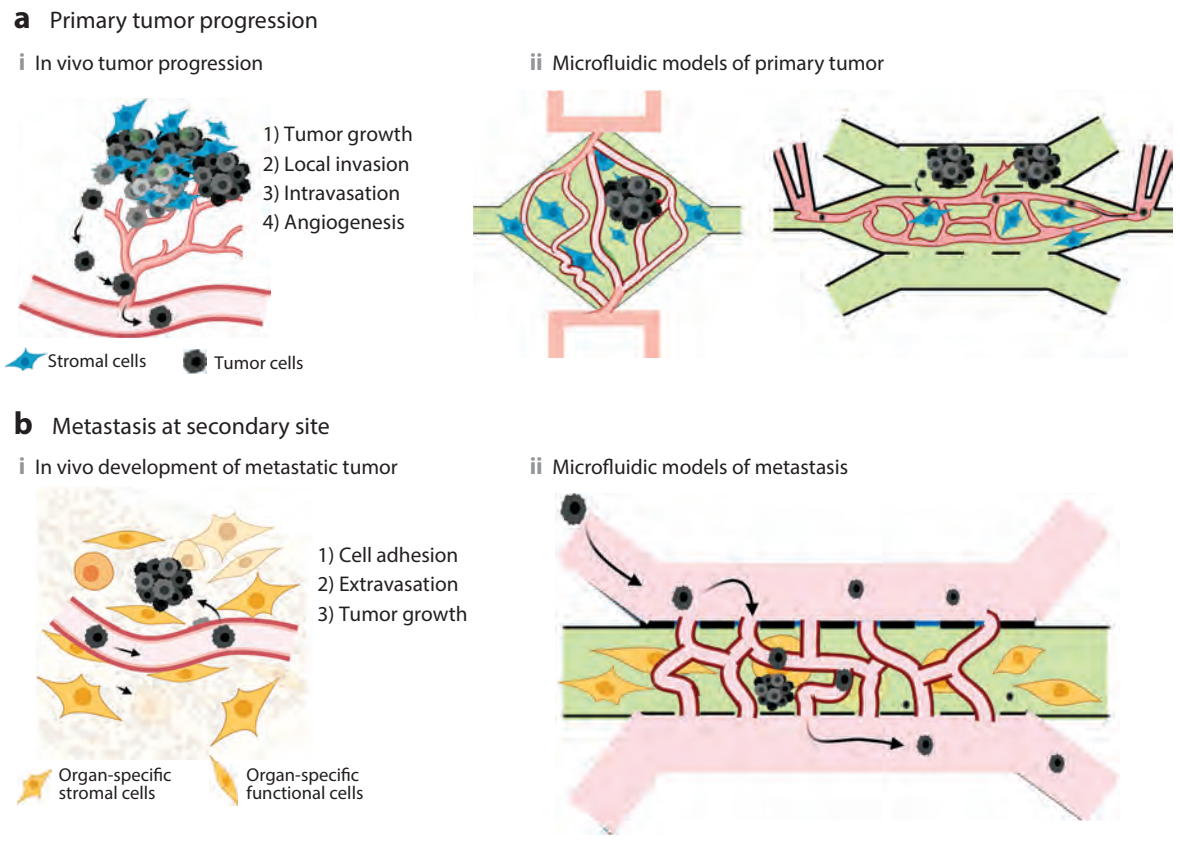

Figure 4

Vascularized organoid models of tumor progression. (*a*) Primary tumor progression. (*i*) Primary tumors grow, invade, intravasate, and stimulate angiogenesis in the surrounding matrix. (*ii*) Several microfluidic models, including the simultaneous coculture of tumor cells, stromal cells, and endothelial cells in a central compartment (*left*), can mimic this process. Alternatively, first the vasculature can be developed within a central compartment over the course of ~1 week, and then tumor cells or spheroids can be seeded in a compartment adjacent to the preformed microvasculature (*right*). (*b*) Metastasis of tumor cells at a distant site. (*i*) Such metastasis involves cell adhesion to the endothelium, extravasation from the vasculature, and growth to form metastatic tumors. (*ii*) An example of a microfluidic device to model this process is creating a vascular network by self-assembly in the presence of organ-specific stromal cells to create an organ-specific microenvironment. Tumor cells can then be introduced in adjacent microfluidic lines and thereafter enter the vascular network. Figure created with BioRender.com.

drug response using 3D vascularized organoids provides exciting opportunities to fill in the gaps between 2D cell culture and in vivo models.

Cancer progression can be divided into the following steps: tumor initiation and growth at the primary site, infiltration of immune cells, angiogenesis, intravasation of primary cancer cells, transit of cancer cells through the vasculature, extravasation of cancer cells at a distant site, and growth of metastatic tumors (**Figure 4*a*,*b***). As such, the tumor microvasculature plays an essential role in tumor progression, as it supplies nutrients to the growing tumor, facilitates immune cell trafficking, and provides a route for cancer cells to disseminate and metastasize. To faithfully recapitulate tumor progression in vitro, organoid models need to include the vasculature.

Early approaches to create 3D vascularized tumor organoids utilized a mixture of tumor cells and ECFC-ECs to create a spheroid and then embedded these spheroids in a 3D gel containing

fibroblasts (121). This strategy allowed the tumor microvasculature to self-assemble. The microvessels penetrated the tumor spheroids, extended into the surrounding matrix, and displayed a different structural phenotype than did nontumor cell controls (121). The vascularized spheroids lacked luminal or interstitial flow, since they were created under static well plate culture conditions. In work from our labs, cancer cells, lung fibroblasts, and ECFC-ECs were mixed in fibrin and seeded in a single chamber of a microfluidic device under physiological interstitial flow conditions; the microvessels formed and connected with the microfluidic lines, generating a perfused microtumor model: the vascularized microtumor (VMT) (**Figure 4*a***). The individual cancer cells in this model proliferated to create microtumors (22), which could then be treated with chemotherapeutics and antiangiogenic drugs through the perfusable vasculature to assess efficacy of the drugs (22). Follow-up studies showed that tumor gene expression in the VMT closely matched that in the same cells in vivo but was quite different from that seen in monolayer cultures or in spheroids (130). In line with this finding, drug responses in the VMT also closely followed those in vivo, but not those in 2D or in spheroids (130). Finally, the TGFβ pathway inhibitor galunisertib, which is in clinical use, was found to be effective in the VMT and in mice, but not in monolayers or spheroids (130).

A potential drawback of this model system, however, is that because the vasculature is formed in parallel with tumor growth, angiogenesis can be studied only after the initial phase of vasculogenesis is complete. Angiogenesis, and not vasculogenesis, is the primary mechanism used by growing tumors to recruit microvessels. In early studies, a single patterned microvessel was used to model tumor angiogenesis (26, 131). When malignant glioblastoma cells (the U87MG cell line) were seeded in a separate compartment, tumor cell–derived soluble factors stimulated vessel sprouting in the microfluidic device (26). In another study, a vessel patterned in collagen gel sprouted only when the collagen was mixed with renal cell carcinoma cells (131). The integrity of the original vessel in this assay was, however, lost because a large number of angiogenic sprouts originated from a single vessel (131). Notably, the microvessels were initially quiescent, were enveloped by a basal membrane, and were partly covered by stromal cells. We have developed an alternative approach to model angiogenesis in the TME that employs the initial self-assembly of a vascular network in a separate compartment, followed by introduction of cancer cells or cancer-secreted factors in an adjacent compartment (**Figure 4*a***). In this strategy, the microvascular network acquires partial pericyte coverage, a basement membrane, and quiescence prior to the introduction of tumor cells (22, 23). Both tumor cell lines and patient-derived tumor organoids have been introduced into the compartment adjacent to the stable perfusable microvascular network. In this system, vessels sprout by angiogenesis toward the tumor to form a vascularized tumor organoid, and drugs can be delivered to the tumor through the vessel network (23). In a recent study, we found distinct EC populations using single-cell RNA sequencing. Interestingly, only ECs in the angiogenic sprouts highly expressed proangiogenic genes (43).

While the process of angiogenesis extends the microvessels toward growing tumors, aggressive tumors also migrate toward microvessels and intravasate to enter the circulation. The migration of tumor cells toward the microvasculature is guided by morphogen gradients and interstitial flow (132). Intravasation of cancer cells into microvessels has been demonstrated in several different microfluidic platforms (23, 133, 134). In a device with separate chambers for tumor cells and self-assembled microvasculature, the tumor cells invaded the vascular chamber, and a small number of cells breached the endothelial barrier (23). Interestingly, the intravasation efficiency of tumor cells was enhanced if the tumor cells were coseeded with macrophages, which increased the permeability of the microvasculature by secreting TNFα (133). A patterned microfluidic channel coated with ECs and separated from tumor cell–containing chambers by a membrane also supported tumor growth and intravasation of tumor cells (134). However, the membrane pores of

these devices are small (<10 μm) (134), and free passage of large cells, such as ECs, can impede angiogenesis.

Multiple microfluidic devices have been established that both contain microvasculature through which tumor cells can be perfused (**Figure 4*b***) and allow for observation of extravasation events with high spatiotemporal resolution (25, 135, 136). To study breast cancer metastasis, a microenvironment of vascularized bone was developed using a self-assembled microvascular network (25, 135). The bone-specific microvascular network was supported by osteodifferentiated primary human bone marrow MSCs, which also secreted bone-specific ECM proteins and generated calcium deposits. The study reported that the extravasation rates of a metastatic breast cancer cell line into the bone microenvironment were four times higher than in a control skeletal muscle microenvironment (25), in line with in vivo observations. An alternate strategy employs a patterned microfluidic channel lined by ECs adjacent to a tumor compartment. By using this strategy to model metastatic brain cancer, a single patterned vessel lined with brain microvascular ECs supported by astrocytes showed low permeability to fluorescent tracers. The integrity of the endothelium was disrupted by lung cancer cells (A549), breast cancer cells (MDA-MB-231), and melanoma cells (M624), but not by liver cancer cells (BEL-7402) (136), consistent with in vivo observations. High-resolution imaging afforded by on-chip devices was used to demonstrate that adhesion of cancer cells via $\alpha_3\beta_1$ and $\alpha_6\beta_1$ integrins to subendothelial laminin is a critical prerequisite for successful extravasation (137).

Immune cells, such as monocytes and macrophages, lymphocytes, and neutrophils, closely interact with cancer cells and ECs and directly impact cancer progression. Vascularized tumor organoid models provide an unprecedented opportunity to investigate and visualize cancer immunology at high spatiotemporal resolution. For example, research has demonstrated that intravascular monocytes directly reduce cancer cell extravasation but that, once monocytes transmigrate through the vasculature, they acquire macrophage-like properties and lose the ability to reduce extravasation (138). In related work, our group recently showed that M1 macrophages, but not M2 macrophages, inhibit angiogenesis and tumor growth of colorectal tumors (43), consistent with in vivo observations (139). In another study, attack of natural killer (NK) cells was mimicked in a vascularized model of cancer in a microfluidic device (140). Antitumor antibodies diffused through the vessels to the TME, but diffusion was substantially hindered by the density of the tumor. In contrast, NK cells could actively transmigrate across the endothelial barrier, penetrate the ECM, and destroy the tumors. The combination of antibody-cytokine conjugates and NK cells led to an enhanced cytotoxicity located mostly at the periphery of the spheroid (140).

FUTURE PERSPECTIVES

The full potential of organ-on-a-chip and organoid technologies will be realized when multiple organ systems with organ-specific microvasculature are physically coupled to allow exchange of cells and fluids. Conditions that require interorgan exchange of fluid and cells can be modeled using integrated systems. Examples of such conditions are physiological and pathological inflammation, autoimmune diseases, allogenic transplants, infections, immune cell therapies, and cancer metastasis. A common feature of these conditions is that paracrine molecules and cells transit through the vasculature and impact the function of distant organs. For example, during infection or cancer, local tissue-specific cells prime immune cells located at distant lymphoid tissues to attract immune cells to the affected tissue. The immune cells must traverse the endothelial barrier and find the target tissue while in transit.

For drug screening applications, multiorgan platforms can mimic absorption, distribution, metabolism, and excretion (ADME) to predict drug efficacy and toxicity more accurately (126,

141, 142). The issue of the relative scaling of various micro-organs in an integrated platform is a critical consideration. Micro-organs can be scaled using power laws, which are created using data across a wide range of living species that relate body and organ masses (143), or can be scaled to match in vivo organ functions, concentrations, or residence time (141, 142). Indeed, a simple coupling approach, in which media from one organ system were manually transferred to another system, generated clinically relevant ADME and toxicity data (100). More complex systems that allow continuous interactions between organ systems via fluidic circuits (144–147) or via periodic exchange of fluid using automated transfer arrangements result in more reliable analysis of pharmacokinetics and toxicity (148). Importantly, the potential use of in vitro–derived pharmacokinetic data to mimic in vivo observations using these coupled systems was recently demonstrated (148).

Nonetheless, to recreate more complex in vivo dynamics, the organ systems must be linked with a dynamic vascular network that can respond (i.e., change vessel caliber or undergo angiogenesis) to changing metabolic needs. Such coupling could be initially achieved by microfluidic lines and later be replaced by larger vasoactive vessels, strategies that have been discussed elsewhere (149). One particularly interesting area of application for integrated systems is immunology. It is notable that animal models cannot mimic all features of the human immunological response (150). An integrated model of lymphoid tissue (e.g., bone marrow, spleen, lymph node) and other organs could model human-specific immune responses and would represent an immediate and a much-needed alternative model to advance our understanding of cancer and inflammation.

DISCLOSURE STATEMENT

C.C.W.H. (Chief Scientific Officer) and S.C.G. are cofounders of Aracari Biosciences, which is commercializing organ-on-a-chip technology. The terms of this arrangement are approved and monitored by the Conflict of Interest Committees at the University of California, Irvine (C.C.W.H.), and the University of California, Davis (S.C.G.). The authors are not aware of any other affiliations, memberships, funding, or financial holdings that might be perceived as affecting the objectivity of this review.

ACKNOWLEDGMENTS

S.C.G. is supported by UG3/UH3 HL141800 and UG3DK122639 from the US National Institutes of Health, by FIP-58 from the Translational Research Institute for Space Health (TRISH), and by C21CR2153 from the Cancer Research Coordinating Committee of the University of California system. C.C.W.H. is supported by UG3/UH3 TR002137, UG3DK122639, and U54 CA217378 and receives support from the Chao Family Comprehensive Cancer Center through National Cancer Institute Center grant P30A062203.

LITERATURE CITED

1. Clevers H. 2016. Modeling development and disease with organoids. *Cell* 165(7):1586–97. **https://doi.org/10.1016/j.cell.2016.05.082**
2. Phan DTT, Wang X, Craver BM, Sobrino A, Zhao D, et al. 2017. A vascularized and perfused organ-on-a-chip platform for large-scale drug screening applications. *Lab Chip* 17(3):511–20. **https://doi.org/10.1039/c6lc01422d**
3. Esch MB, Ueno H, Applegate DR, Shuler ML. 2016. Modular, pumpless body-on-a-chip platform for the co-culture of GI tract epithelium and 3D primary liver tissue. *Lab Chip* 16(14):2719–29. **https://doi.org/10.1039/c6lc00461j**

4. Jain RK, Au P, Tam J, Duda DG, Fukumura D. 2005. Engineering vascularized tissue. *Nat. Biotechnol.* 23(7):821–23. **https://doi.org/10.1038/nbt0705-821**
5. Daniel E, Cleaver O. 2019. Vascularizing organogenesis: lessons from developmental biology and implications for regenerative medicine. *Curr. Top. Dev. Biol.* 132:177–220. **https://doi.org/10.1016/bs.ctdb.2018.12.012**
6. Nakatsu MN, Hughes CCW. 2008. An optimized three-dimensional in vitro model for the analysis of angiogenesis. *Methods Enzymol.* 443:65–82. **https://doi.org/10.1016/S0076-6879(08)02004-1**
7. Welch-Reardon KM, Ehsan SM, Wang KH, Wu N, Newman AC, et al. 2014. Angiogenic sprouting is regulated by endothelial cell expression of Slug. *J. Cell Sci.* 127(9):2017–28. **https://doi.org/10.1242/jcs.143420**
8. Chrobak KM, Potter DR, Tien J. 2006. Formation of perfused, functional microvascular tubes in vitro. *Microvasc. Res.* 71(3):185–96. **https://doi.org/10.1016/j.mvr.2006.02.005**
9. Song JW, Munn LL. 2011. Fluid forces control endothelial sprouting. *PNAS* 108(37):15342–47. **https://doi.org/10.1073/pnas.1105316108**
10. Huh D, Matthews BD, Mammoto A, Montoya-Zavala M, Hsin HY, Ingber DE. 2010. Reconstituting organ-level lung functions on a chip. *Science* 328(5986):1662–68. **https://doi.org/10.1126/science.1188302**
11. Zheng Y, Chen J, Craven M, Choi NW, Totorica S, et al. 2012. In vitro microvessels for the study of angiogenesis and thrombosis. *PNAS* 109(24):9342–47. **https://doi.org/10.1073/pnas.1201240109**
12. Bischel LL, Young EWK, Mader BR, Beebe DJ. 2013. Tubeless microfluidic angiogenesis assay with three-dimensional endothelial-lined microvessels. *Biomaterials* 34(5):1471–77. **https://doi.org/10.1016/j.biomaterials.2012.11.005**
13. Miller JS, Stevens KR, Yang MT, Baker BM, Nguyen DH, et al. 2012. Rapid casting of patterned vascular networks for perfusable engineered three-dimensional tissues. *Nat. Mater.* 11(9):768–74. **https://doi.org/10.1038/nmat3357**
14. Verbridge SS, Chakrabarti A, DelNero P, Kwee B, Varner JD, et al. 2013. Physicochemical regulation of endothelial sprouting in a 3D microfluidic angiogenesis model. *J. Biomed. Mater. Res. A* 101(10):2948–56. **https://doi.org/10.1002/jbm.a.34587**
15. Fisher AB, Chien S, Barakat AI, Nerem RM. 2001. Endothelial cellular response to altered shear stress. *Am. J. Physiol. Lung Cell. Mol. Physiol.* 281(3):L529–33. **https://doi.org/10.1152/ajplung.2001.281.3.L529**
16. Atkins GB, Jain MK. 2007. Role of Krüppel-like transcription factors in endothelial biology. *Circ. Res.* 100(12):1686–95. **https://doi.org/10.1161/01.res.0000267856.00713.0a**
17. Haase K, Kamm RD. 2017. Advances in on-chip vascularization. *Regen. Med.* 12(3):285–302. **https://doi.org/10.2217/rme-2016-0152**
18. Bogorad MI, Destefano J, Karlsson J, Wong AD, Gerecht S, Searson PC. 2015. In vitro microvessel models. *Lab Chip* 15(22):4242–55. **https://doi.org/10.1039/c5lc00832h**
19. Grebenyuk S, Ranga A. 2019. Engineering organoid vascularization. *Front. Bioeng. Biotechnol.* 7:39. **https://doi.org/10.3389/fbioe.2019.00039**
20. Melero-Martin JM, Khan ZA, Picard A, Wu X, Paruchuri S, Bischoff J. 2007. In vivo vasculogenic potential of human blood-derived endothelial progenitor cells. *Blood* 109(11):4761–68. **https://doi.org/10.1182/blood-2006-12-062471**
21. Yoon CH, Hur J, Park KW, Kim JH, Lee CS, et al. 2005. Synergistic neovascularization by mixed transplantation of early endothelial progenitor cells and late outgrowth endothelial cells: the role of angiogenic cytokines and matrix metalloproteinases. *Circulation* 112(11):1618–27. **https://doi.org/10.1161/CIRCULATIONAHA.104.503433**
22. Sobrino A, Phan DTT, Datta R, Wang X, Hachey SJ, et al. 2016. 3D microtumors in vitro supported by perfused vascular networks. *Sci. Rep.* 6(1):31589. **https://doi.org/10.1038/srep31589**
23. Shirure VS, Bi Y, Curtis MB, Lezia A, Goedegebuure MM, et al. 2018. Tumor-on-a-chip platform to investigate progression and drug sensitivity in cell lines and patient-derived organoids. *Lab Chip* 18(23):3687–702. **https://doi.org/10.1039/c8lc00596f**
24. Moya ML, Hsu Y-H, Lee AP, Hughes CCW, George SC. 2013. In vitro perfused human capillary networks. *Tissue Eng. C* 19(9):730–37. **https://doi.org/10.1089/ten.tec.2012.0430**

25. Jeon JS, Bersini S, Gilardi M, Dubini G, Charest JL, et al. 2015. Human 3D vascularized organotypic microfluidic assays to study breast cancer cell extravasation. *PNAS* 112(1):214–19. **https://doi.org/10.1073/pnas.1417115112**
26. Kim S, Lee H, Chung M, Jeon NL. 2013. Engineering of functional, perfusable 3D microvascular networks on a chip. *Lab Chip* 13(8):1489–500. **https://doi.org/10.1039/c3lc41320a**
27. Nashimoto Y, Hayashi T, Kunita I, Nakamasu A, Torisawa Y-S, et al. 2017. Integrating perfusable vascular networks with a three-dimensional tissue in a microfluidic device. *Integr. Biol.* 9(6):506–18. **https://doi.org/10.1039/c7ib00024c**
28. Song HHG, Lammers A, Sundaram S, Rubio L, Chen AX, et al. 2020. Transient support from fibroblasts is sufficient to drive functional vascularization in engineered tissues. *Adv. Funct. Mater.* 2020:2003777. **https://doi.org/10.1002/adfm.202003777**
29. Wang X, Phan DT, Sobrino A, George SC, Hughes CC, Lee AP. 2016. Engineering anastomosis between living capillary networks and endothelial cell–lined microfluidic channels. *Lab Chip* 16(2):282–90. **https://doi.org/10.1039/c5lc01050k**
30. Newman AC, Chou W, Welch-Reardon KM, Fong AH, Popson SA, et al. 2013. Analysis of stromal cell secretomes reveals a critical role for stromal cell–derived hepatocyte growth factor and fibronectin in angiogenesis. *Arterioscler. Thromb. Vasc. Biol.* 33(3):513–22. **https://doi.org/10.1161/ATVBAHA.112.300782**
31. Newman AC, Nakatsu MN, Chou W, Gershon PD, Hughes CC. 2011. The requirement for fibroblasts in angiogenesis: Fibroblast-derived matrix proteins are essential for endothelial cell lumen formation. *Mol. Biol. Cell* 22(20):3791–800. **https://doi.org/10.1091/mbc.E11-05-0393**
32. Chen X, Aledia AS, Popson SA, Him L, Hughes CCW, George SC. 2010. Rapid anastomosis of endothelial progenitor cell–derived vessels with host vasculature is promoted by a high density of cotransplanted fibroblasts. *Tissue Eng. A* 16(2):585–94. **https://doi.org/10.1089/ten.tea.2009.0491**
33. Au P, Daheron LM, Duda DG, Cohen KS, Tyrrell JA, et al. 2008. Differential in vivo potential of endothelial progenitor cells from human umbilical cord blood and adult peripheral blood to form functional long-lasting vessels. *Blood* 111(3):1302–5. **https://doi.org/10.1182/blood-2007-06-094318**
34. De Masi C, Spitalieri P, Murdocca M, Novelli G, Sangiuolo F. 2020. Application of CRISPR/Cas9 to human induced pluripotent stem cells: from gene editing to drug discovery. *Hum. Genom.* 14(1):25. **https://doi.org/10.1186/s40246-020-00276-2**
35. Samuel R, Daheron L, Liao S, Vardam T, Kamoun WS, et al. 2013. Generation of functionally competent and durable engineered blood vessels from human induced pluripotent stem cells. *PNAS* 110(31):12774–79. **https://doi.org/10.1073/pnas.1310675110**
36. Patsch C, Challet-Meylan L, Thoma EC, Urich E, Heckel T, et al. 2015. Generation of vascular endothelial and smooth muscle cells from human pluripotent stem cells. *Nat. Cell Biol.* 17(8):994–1003. **https://doi.org/10.1038/ncb3205**
37. Kurokawa YK, Yin RT, Shang MR, Shirure VS, Moya ML, George SC. 2017. Human induced pluripotent stem cell–derived endothelial cells for three-dimensional microphysiological systems. *Tissue Eng. C* 23(8):474–84. **https://doi.org/10.1089/ten.tec.2017.0133**
38. Kusuma S, Shen YI, Hanjaya-Putra D, Mali P, Cheng L, Gerecht S. 2013. Self-organized vascular networks from human pluripotent stem cells in a synthetic matrix. *PNAS* 110(31):12601–6. **https://doi.org/10.1073/pnas.1306562110**
39. Marcu R, Choi YJ, Xue J, Fortin CL, Wang Y, et al. 2018. Human organ–specific endothelial cell heterogeneity. *iScience* 4:20–35. **https://doi.org/10.1016/j.isci.2018.05.003**
40. Nolan DJ, Ginsberg M, Israely E, Palikuqi B, Poulos MG, et al. 2013. Molecular signatures of tissue-specific microvascular endothelial cell heterogeneity in organ maintenance and regeneration. *Dev. Cell* 26(2):204–19. **https://doi.org/10.1016/j.devcel.2013.06.017**
41. Herron LA, Hansen CS, Abaci HE. 2019. Engineering tissue-specific blood vessels. *Bioeng. Transl. Med.* 4(3):e10139. **https://doi.org/10.1002/btm2.10139**
42. Marino D, Luginbuhl J, Scola S, Meuli M, Reichmann E. 2014. Bioengineering dermo-epidermal skin grafts with blood and lymphatic capillaries. *Sci. Transl. Med.* 6(221):221ra14. **https://doi.org/10.1126/scitranslmed.3006894**

43. Bi Y, Shirure VS, Liu R, Cunningham C, Ding L, et al. 2020. Tumor-on-a-chip platform to interrogate the role of macrophages in tumor progression. *Integr. Biol.* 12(9):221–32. **https://doi.org/10.1093/intbio/zyaa017**
44. Griffith CK, Miller C, Sainson RC, Calvert JW, Jeon NL, et al. 2005. Diffusion limits of an in vitro thick prevascularized tissue. *Tissue Eng.* 11(1–2):257–66
45. Hughes CC. 2008. Endothelial–stromal interactions in angiogenesis. *Curr. Opin. Hematol.* 15(3):204–9. **https://doi.org/10.1097/moh.0b013e3282f97dbc**
46. Sewell-Loftin MK, Bayer SVH, Crist E, Hughes T, Joison SM, et al. 2017. Cancer-associated fibroblasts support vascular growth through mechanical force. *Sci. Rep.* 7(1):12574. **https://doi.org/10.1038/s41598-017-13006-x**
47. Ghajar CM, Blevins KS, Hughes CC, George SC, Putnam AJ. 2006. Mesenchymal stem cells enhance angiogenesis in mechanically viable prevascularized tissues via early matrix metalloproteinase upregulation. *Tissue Eng.* 12(10):2875–88. **https://doi.org/10.1089/ten.2006.12.2875**
48. Orlova VV, van den Hil FE, Petrus-Reurer S, Drabsch Y, Ten Dijke P, Mummery CL. 2014. Generation, expansion and functional analysis of endothelial cells and pericytes derived from human pluripotent stem cells. *Nat. Protoc.* 9(6):1514–31. **https://doi.org/10.1038/nprot.2014.102**
49. Swartz MA, Fleury ME. 2007. Interstitial flow and its effects in soft tissues. *Annu. Rev. Biomed. Eng.* 9:229–56. **https://doi.org/10.1146/annurev.bioeng.9.060906.151850**
50. Shirure VS, Lezia A, Tao A, Alonzo LF, George SC. 2017. Low levels of physiological interstitial flow eliminate morphogen gradients and guide angiogenesis. *Angiogenesis* 20(4):493–504. **https://doi.org/10.1007/s10456-017-9559-4**
51. Hsu YH, Moya ML, Abiri P, Hughes CC, George SC, Lee AP. 2013. Full range physiological mass transport control in 3D tissue cultures. *Lab Chip* 13(1):81–89. **https://doi.org/10.1039/c2lc40787f**
52. Galie PA, Nguyen DH, Choi CK, Cohen DM, Janmey PA, Chen CS. 2014. Fluid shear stress threshold regulates angiogenic sprouting. *PNAS* 111(22):7968–73. **https://doi.org/10.1073/pnas.1310842111**
53. Polacheck WJ, German AE, Mammoto A, Ingber DE, Kamm RD. 2014. Mechanotransduction of fluid stresses governs 3D cell migration. *PNAS* 111(7):2447–52. **https://doi.org/10.1073/pnas.1316848111**
54. Ghajar CM, Chen X, Harris JW, Suresh V, Hughes CC, et al. 2008. The effect of matrix density on the regulation of 3-D capillary morphogenesis. *Biophys. J.* 94(5):1930–41
55. Shamloo A, Heilshorn SC. 2010. Matrix density mediates polarization and lumen formation of endothelial sprouts in VEGF gradients. *Lab Chip* 10(22):3061–68. **https://doi.org/10.1039/c005069e**
56. Crosby CO, Zoldan J. 2019. Mimicking the physical cues of the ECM in angiogenic biomaterials. *Regen. Biomater.* 6(2):61–73. **https://doi.org/10.1093/rb/rbz003**
57. Osaki T, Sivathanu V, Kamm RD. 2018. Engineered 3D vascular and neuronal networks in a microfluidic platform. *Sci. Rep.* 8(1):5168. **https://doi.org/10.1038/s41598-018-23512-1**
58. Badylak S, Freytes D, Gilbert T. 2009. Extracellular matrix as a biological scaffold material: structure and function. *Acta Biomater.* 5(1):1–13. **https://doi.org/10.1016/j.actbio.2008.09.013**
59. Romero-Lopez M, Trinh AL, Sobrino A, Hatch MM, Keating MT, et al. 2017. Recapitulating the human tumor microenvironment: Colon tumor–derived extracellular matrix promotes angiogenesis and tumor cell growth. *Biomaterials* 116:118–29. **https://doi.org/10.1016/j.biomaterials.2016.11.034**
60. Natividad-Diaz SL, Browne S, Jha AK, Ma Z, Hossainy S, et al. 2019. A combined hiPSC-derived endothelial cell and in vitro microfluidic platform for assessing biomaterial-based angiogenesis. *Biomaterials* 194:73–83. **https://doi.org/10.1016/j.biomaterials.2018.11.032**
61. Wenz A, Tjoeng I, Schneider I, Kluger PJ, Borchers K. 2018. Improved vasculogenesis and bone matrix formation through coculture of endothelial cells and stem cells in tissue-specific methacryloyl gelatin–based hydrogels. *Biotechnol. Bioeng.* 115(10):2643–53. **https://doi.org/10.1002/bit.26792**
62. Zhang B, Montgomery M, Chamberlain MD, Ogawa S, Korolj A, et al. 2016. Biodegradable scaffold with built-in vasculature for organ-on-a-chip engineering and direct surgical anastomosis. *Nat. Mater.* 15(6):669–78. **https://doi.org/10.1038/nmat4570**
63. Torisawa YS, Spina CS, Mammoto T, Mammoto A, Weaver JC, et al. 2014. Bone marrow–on–a–chip replicates hematopoietic niche physiology in vitro. *Nat. Methods* 11(6):663–69. **https://doi.org/10.1038/nmeth.2938**

64. Correia C, Grayson WL, Park M, Hutton D, Zhou B, et al. 2011. In vitro model of vascularized bone: synergizing vascular development and osteogenesis. *PLOS ONE* 6(12):e28352. **https://doi.org/10.1371/journal.pone.0028352**
65. Marturano-Kruik A, Nava MM, Yeager K, Chramiec A, Hao L, et al. 2018. Human bone perivascular niche-on-a-chip for studying metastatic colonization. *PNAS* 115(6):1256–61. **https://doi.org/10.1073/pnas.1714282115**
66. Bersini S, Jeon JS, Dubini G, Arrigoni C, Chung S, et al. 2014. A microfluidic 3D in vitro model for specificity of breast cancer metastasis to bone. *Biomaterials* 35(8):2454–61. **https://doi.org/10.1016/j.biomaterials.2013.11.050**
67. Chou DB, Frismantas V, Milton Y, David R, Pop-Damkov P, et al. 2020. On-chip recapitulation of clinical bone marrow toxicities and patient-specific pathophysiology. *Nat. Biomed. Eng.* 394–406. **https://doi.org/10.1038/s41551-019-0495-z**
68. Sieber S, Wirth L, Cavak N, Koenigsmark M, Marx U, et al. 2018. Bone marrow-on-a-chip: long-term culture of human haematopoietic stem cells in a three-dimensional microfluidic environment. *J. Tissue Eng. Regen. Med.* 12(2):479–89. **https://doi.org/10.1002/term.2507**
69. Glaser DE, Curtis MB, Sariano PA, Rollins ZA, Shergill BS, et al. 2020. Organ-on-a-chip model of vascularized human bone marrow niches. bioRxiv 2020.04.17.039339. **https://doi.org/10.1101/2020.04.17.039339**
70. Phan DT, Bender RHF, Andrejecsk JW, Sobrino A, Hachey SJ, et al. 2017. Blood-brain barrier-on-a-chip: microphysiological systems that capture the complexity of the blood–central nervous system interface. *Exp. Biol. Med.* 242(17):1669–78. **https://doi.org/10.1177/1535370217694100**
71. Wang YI, Abaci HE, Shuler ML. 2017. Microfluidic blood-brain barrier model provides in vivo–like barrier properties for drug permeability screening. *Biotechnol. Bioeng.* 114(1):184–94. **https://doi.org/10.1002/bit.26045**
72. Brown JA, Pensabene V, Markov DA, Allwardt V, Neely MD, et al. 2015. Recreating blood-brain barrier physiology and structure on chip: a novel neurovascular microfluidic bioreactor. *Biomicrofluidics* 9(5):054124. **https://doi.org/10.1063/1.4934713**
73. Herland A, van der Meer AD, FitzGerald EA, Park TE, Sleeboom JJ, Ingber DE. 2016. Distinct contributions of astrocytes and pericytes to neuroinflammation identified in a 3D human blood-brain barrier on a chip. *PLOS ONE* 11(3):e0150360. **https://doi.org/10.1371/journal.pone.0150360**
74. Lippmann ES, Azarin SM, Kay JE, Nessler RA, Wilson HK, et al. 2012. Derivation of blood-brain barrier endothelial cells from human pluripotent stem cells. *Nat. Biotechnol.* 30(8):783–91. **https://doi.org/10.1038/nbt.2247**
75. Wolff A, Antfolk M, Brodin B, Tenje M. 2015. In vitro blood–brain barrier models—an overview of established models and new microfluidic approaches. *J. Pharm. Sci.* 104(9):2727–46. **https://doi.org/10.1002/jps.24329**
76. Campisi M, Shin Y, Osaki T, Hajal C, Chiono V, Kamm RD. 2018. 3D self-organized microvascular model of the human blood-brain barrier with endothelial cells, pericytes and astrocytes. *Biomaterials* 180:117–29. **https://doi.org/10.1016/j.biomaterials.2018.07.014**
77. Canfield SG, Stebbins MJ, Morales BS, Asai SW, Vatine GD, et al. 2017. An isogenic blood-brain barrier model comprising brain endothelial cells, astrocytes, and neurons derived from human induced pluripotent stem cells. *J. Neurochem.* 140(6):874–88. **https://doi.org/10.1111/jnc.13923**
78. Schwartz MP, Hou Z, Propson NE, Zhang J, Engstrom CJ, et al. 2015. Human pluripotent stem cell–derived neural constructs for predicting neural toxicity. *PNAS* 112(40):12516–21. **https://doi.org/10.1073/pnas.1516645112**
79. Maoz BM, Herland A, Fitzgerald EA, Grevesse T, Vidoudez C, et al. 2018. A linked organ-on-chip model of the human neurovascular unit reveals the metabolic coupling of endothelial and neuronal cells. *Nat. Biotechnol.* 36(9):865–74. **https://doi.org/10.1038/nbt.4226**
80. Aird WC. 2007. Phenotypic heterogeneity of the endothelium. *Circ. Res.* 100(2):174–90. **https://doi.org/10.1161/01.res.0000255690.03436.ae**
81. Mummery CL, Zhang J, Ng ES, Elliott DA, Elefanty AG, Kamp TJ. 2012. Differentiation of human embryonic stem cells and induced pluripotent stem cells to cardiomyocytes: a methods overview. *Circ. Res.* 111(3):344–58. **https://doi.org/10.1161/CIRCRESAHA.110.227512**

82. Ronaldson-Bouchard K, Ma SP, Yeager K, Chen T, Song L, et al. 2018. Advanced maturation of human cardiac tissue grown from pluripotent stem cells. *Nature* 556(7700):239–43. **https://doi.org/10.1038/s41586-018-0016-3**
83. Fong AH, Romero-Lopez M, Heylman CM, Keating M, Tran D, et al. 2016. Three-dimensional adult cardiac extracellular matrix promotes maturation of human induced pluripotent stem cell–derived cardiomyocytes. *Tissue Eng. A* 22(15–16):1016–25. **https://doi.org/10.1089/ten.TEA.2016.0027**
84. Sekine H, Shimizu T, Hobo K, Sekiya S, Yang J, et al. 2008. Endothelial cell coculture within tissue-engineered cardiomyocyte sheets enhances neovascularization and improves cardiac function of ischemic hearts. *Circulation* 118(14 Suppl. 1):145–52. **https://doi.org/10.1161/circulationaha.107.757286**
85. Caspi O, Lesman A, Basevitch Y, Gepstein A, Arbel G, et al. 2007. Tissue engineering of vascularized cardiac muscle from human embryonic stem cells. *Circ. Res.* 100(2):263–72. **https://doi.org/10.1161/01.res.0000257776.05673.ff**
86. Kurokawa YK, Shang MR, Yin RT, George SC. 2018. Modeling trastuzumab-related cardiotoxicity in vitro using human stem cell–derived cardiomyocytes. *Toxicol. Lett.* 285:74–80. **https://doi.org/10.1016/j.toxlet.2018.01.001**
87. Polonchuk L, Chabria M, Badi L, Hoflack J-C, Figtree G, et al. 2017. Cardiac spheroids as promising in vitro models to study the human heart microenvironment. *Sci. Rep.* 7(1):7005. **https://doi.org/10.1038/s41598-017-06385-8**
88. Arai K, Murata D, Verissimo AR, Mukae Y, Itoh M, et al. 2018. Fabrication of scaffold-free tubular cardiac constructs using a Bio-3D printer. *PLOS ONE* 13(12):e0209162. **https://doi.org/10.1371/journal.pone.0209162**
89. Weng K-C, Kurokawa YK, Hajek BS, Paladin JA, Shirure VS, George SC. 2020. Human induced pluripotent stem-cardiac-endothelial-tumor-on-a-chip to assess anticancer efficacy and cardiotoxicity. *Tissue Eng. C* 26(1):44–55. **https://doi.org/10.1089/ten.tec.2019.0248**
90. Pepper AR, Gala-Lopez B, Ziff O, Shapiro AMJ. 2013. Revascularization of transplanted pancreatic islets and role of the transplantation site. *Clin. Dev. Immunol.* 2013:352315. **https://doi.org/10.1155/2013/352315**
91. Vlahos AE, Cober N, Sefton MV. 2017. Modular tissue engineering for the vascularization of subcutaneously transplanted pancreatic islets. *PNAS* 114(35):9337–42. **https://doi.org/10.1073/pnas.1619216114**
92. Jun Y, Lee J, Choi S, Yang JH, Sander M, et al. 2019. In vivo–mimicking microfluidic perfusion culture of pancreatic islet spheroids. *Sci. Adv.* 5(11):eaax4520. **https://doi.org/10.1126/sciadv.aax4520**
93. Rambol MH, Han E, Niklason LE. 2020. Microvessel network formation and interactions with pancreatic islets in three-dimensional chip cultures. *Tissue Eng. A* 26(9–10):556–68. **https://doi.org/10.1089/ten.TEA.2019.0186**
94. Takebe T, Sekine K, Enomura M, Koike H, Kimura M, et al. 2013. Vascularized and functional human liver from an iPSC-derived organ bud transplant. *Nature* 499(7459):481–84. **https://doi.org/10.1038/nature12271**
95. Takebe T, Koike N, Sekine K, Fujiwara R, Amiya T, et al. 2014. Engineering of human hepatic tissue with functional vascular networks. *Organogenesis* 10(2):260–67. **https://doi.org/10.4161/org.27590**
96. Ribeiro AJS, Yang X, Patel V, Madabushi R, Strauss DG. 2019. Liver microphysiological systems for predicting and evaluating drug effects. *Clin. Pharmacol. Ther.* 106(1):139–47. **https://doi.org/10.1002/cpt.1458**
97. Sasaki K, Akagi T, Asaoka T, Eguchi H, Fukuda Y, et al. 2017. Construction of three-dimensional vascularized functional human liver tissue using a layer-by-layer cell coating technique. *Biomaterials* 133:263–74. **https://doi.org/10.1016/j.biomaterials.2017.02.034**
98. Lee JW, Choi YJ, Yong WJ, Pati F, Shim JH, et al. 2016. Development of a 3D cell printed construct considering angiogenesis for liver tissue engineering. *Biofabrication* 8(1):015007. **https://doi.org/10.1088/1758-5090/8/1/015007**
99. Vernetti LA, Senutovitch N, Boltz R, DeBiasio R, Shun TY, et al. 2016. A human liver microphysiology platform for investigating physiology, drug safety, and disease models. *Exp. Biol. Med.* 241(1):101–14. **https://doi.org/10.1177/1535370215592121**

100. Vernetti L, Gough A, Baetz N, Blutt S, Broughman JR, et al. 2017. Functional coupling of human microphysiology systems: intestine, liver, kidney proximal tubule, blood-brain barrier and skeletal muscle. *Sci. Rep.* 7(1):42296. **https://doi.org/10.1038/srep42296**
101. Spence JR, Mayhew CN, Rankin SA, Kuhar MF, Vallance JE, et al. 2011. Directed differentiation of human pluripotent stem cells into intestinal tissue in vitro. *Nature* 470(7332):105–9. **https://doi.org/10.1038/nature09691**
102. Watson CL, Mahe MM, Múnera J, Howell JC, Sundaram N, et al. 2014. An in vivo model of human small intestine using pluripotent stem cells. *Nat. Med.* 20(11):1310–14. **https://doi.org/10.1038/nm.3737**
103. Kitano K, Schwartz DM, Zhou H, Gilpin SE, Wojtkiewicz GR, et al. 2017. Bioengineering of functional human induced pluripotent stem cell–derived intestinal grafts. *Nat. Commun.* 8(1):765. **https://doi.org/10.1038/s41467-017-00779-y**
104. Seiler KM, Bajinting A, Alvarado DM, Traore MA, Binkley MM, et al. 2020. Patient-derived small intestinal myofibroblasts direct perfused, physiologically responsive capillary development in a microfluidic Gut-on-a-Chip Model. *Sci. Rep.* 10(1):3842. **https://doi.org/10.1038/s41598-020-60672-5**
105. Kasendra M, Tovaglieri A, Sontheimer-Phelps A, Jalili-Firoozinezhad S, Bein A, et al. 2018. Development of a primary human Small Intestine–on–a–Chip using biopsy-derived organoids. *Sci. Rep.* 8(1):2871. **https://doi.org/10.1038/s41598-018-21201-7**
106. Jalili-Firoozinezhad S, Gazzaniga FS, Calamari EL, Camacho DM, Fadel CW, et al. 2019. A complex human gut microbiome cultured in an anaerobic intestine-on-a-chip. *Nat. Biomed. Eng.* 3(7):520–31. **https://doi.org/10.1038/s41551-019-0397-0**
107. Takasato M, Er PX, Chiu HS, Maier B, Baillie GJ, et al. 2015. Kidney organoids from human iPS cells contain multiple lineages and model human nephrogenesis. *Nature* 526(7574):564–68. **https://doi.org/10.1038/nature15695**
108. Yeung CK, Himmelfarb J. 2019. Kidneys on chips. *Clin. J. Am. Soc. Nephrol.* 14(1):144–46. **https://doi.org/10.2215/cjn.06690518**
109. Jang K-J, Mehr AP, Hamilton GA, McPartlin LA, Chung S, et al. 2013. Human kidney proximal tubule–on–a–chip for drug transport and nephrotoxicity assessment. *Integr. Biol.* 5(9):1119–29. **https://doi.org/10.1039/c3ib40049b**
110. Weber EJ, Chapron A, Chapron BD, Voellinger JL, Lidberg KA, et al. 2016. Development of a microphysiological model of human kidney proximal tubule function. *Kidney Int.* 90(3):627–37. **https://doi.org/10.1016/j.kint.2016.06.011**
111. Petrosyan A, Cravedi P, Villani V, Angeletti A, Manrique J, et al. 2019. A glomerulus-on-a-chip to recapitulate the human glomerular filtration barrier. *Nat. Commun.* 10(1):3656. **https://doi.org/10.1038/s41467-019-11577-z**
112. Ligresti G, Nagao RJ, Xue J, Choi YJ, Xu J, et al. 2016. A novel three-dimensional human peritubular microvascular system. *J. Am. Soc. Nephrol.* 27(8):2370–81. **https://doi.org/10.1681/ASN.2015070747**
113. Benam KH, Villenave R, Lucchesi C, Varone A, Hubeau C, et al. 2016. Small airway-on-a-chip enables analysis of human lung inflammation and drug responses in vitro. *Nat. Methods* 13(2):151–57. **https://doi.org/10.1038/nmeth.3697**
114. Huh D, Leslie DC, Matthews BD, Fraser JP, Jurek S, et al. 2012. A human disease model of drug toxicity–induced pulmonary edema in a lung-on-a-chip microdevice. *Sci. Transl. Med.* 4(159):159ra47–ra1. **https://doi.org/10.1126/scitranslmed.3004249**
115. Huang SXL, Islam MN, O'Neill J, Hu Z, Yang Y-G, et al. 2014. Efficient generation of lung and airway epithelial cells from human pluripotent stem cells. *Nat. Biotechnol.* 32(1):84–91. **https://doi.org/10.1038/nbt.2754**
116. Dye BR, Hill DR, Ferguson MA, Tsai Y-H, Nagy MS, et al. 2015. In vitro generation of human pluripotent stem cell derived lung organoids. *eLife* 4:05098. **https://doi.org/10.7554/elife.05098**
117. Thompson HG, Truong DT, Griffith CK, George SC. 2007. A three-dimensional in vitro model of angiogenesis in the airway mucosa. *Pulm. Pharmacol. Ther.* 20(2):141–48. **https://doi.org/10.1016/j.pupt.2005.12.001**
118. Tan Q, Choi KM, Sicard D, Tschumperlin DJ. 2017. Human airway organoid engineering as a step toward lung regeneration and disease modeling. *Biomaterials* 113:118–32. **https://doi.org/10.1016/j.biomaterials.2016.10.046**

119. Shirure VS, Ye B, Curtis MB, Lezia A, Goedegebuure MM, et al. 2018. Tumor-on-a-chip platform to investigate progression and drug sensitivity in cell lines and patient-derived organoids. *Lab Chip* 18(23):3687–702. **https://doi.org/10.1039/c8lc00596f**
120. Lee H, Park W, Ryu H, Jeon NL. 2014. A microfluidic platform for quantitative analysis of cancer angiogenesis and intravasation. *Biomicrofluidics* 8(5):054102. **https://doi.org/10.1063/1.4894595**
121. Ehsan SM, Welch-Reardon KM, Waterman ML, Hughes CCW, George SC. 2014. A three-dimensional in vitro model of tumor cell intravasation. *Integr. Biol.* 6(6):603–10. **https://doi.org/10.1039/c3ib40170g**
122. David L, Dulong V, Le Cerf D, Cazin L, Lamacz M, Vannier JP. 2008. Hyaluronan hydrogel: an appropriate three-dimensional model for evaluation of anticancer drug sensitivity. *Acta Biomater.* 4(2):256–63. **https://doi.org/10.1016/j.actbio.2007.08.012**
123. Gurski LA, Jha AK, Zhang C, Jia X, Farach-Carson MC. 2009. Hyaluronic acid–based hydrogels as 3D matrices for in vitro evaluation of chemotherapeutic drugs using poorly adherent prostate cancer cells. *Biomaterials* 30(30):6076–85. **https://doi.org/10.1016/j.biomaterials.2009.07.054**
124. Serebriiskii I, Castello-Cros R, Lamb A, Golemis EA, Cukierman E. 2008. Fibroblast-derived 3D matrix differentially regulates the growth and drug-responsiveness of human cancer cells. *Matrix Biol.* 27(6):573–85. **https://doi.org/10.1016/j.matbio.2008.02.008**
125. Weigelt B, Lo AT, Park CC, Gray JW, Bissell MJ. 2010. HER2 signaling pathway activation and response of breast cancer cells to HER2-targeting agents is dependent strongly on the 3D microenvironment. *Breast Cancer Res. Treat.* 122(1):35–43. **https://doi.org/10.1007/s10549-009-0502-2**
126. Heylman C, Sobrino A, Shirure VS, Hughes CC, George SC. 2014. A strategy for integrating essential three-dimensional microphysiological systems of human organs for realistic anticancer drug screening. *Exp. Biol. Med.* 239(9):1240–54. **https://doi.org/10.1177/1535370214525295**
127. Baginska J, Viry E, Paggetti J, Medves S, Berchem G, et al. 2013. The critical role of the tumor microenvironment in shaping natural killer cell–mediated anti-tumor immunity. *Front. Immunol.* 4:490. **https://doi.org/10.3389/fimmu.2013.00490**
128. Blonska M, Agarwal NK, Vega F. 2015. Shaping of the tumor microenvironment: stromal cells and vessels. *Semin. Cancer Biol.* 34:3–13. **https://doi.org/10.1016/j.semcancer.2015.03.002**
129. McAllister SS, Weinberg RA. 2014. The tumour-induced systemic environment as a critical regulator of cancer progression and metastasis. *Nat. Cell Biol.* 16(8):717–27. **https://doi.org/10.1038/ncb3015**
130. Hachey SJ, Movsesyan S, Nguyen QH, Burton-Sojo G, Tankanzyan A, et al. 2020. An in vitro vascularized micro-tumor model of human colorectal cancer recapitulates in vivo drug responses. bioRxiv 2020.03.03.973891. **https://doi.org/10.1101/2020.03.03.973891**
131. Miller CP, Tsuchida C, Zheng Y, Himmelfarb J, Akilesh S. 2018. A 3D human renal cell carcinoma-on-a-chip for the study of tumor angiogenesis. *Neoplasia* 20(6):610–20. **https://doi.org/10.1016/j.neo.2018.02.011**
132. Griffith LG, Swartz MA. 2006. Capturing complex 3D tissue physiology in vitro. *Nat. Rev. Mol. Cell Biol.* 7(3):211–24. **https://doi.org/10.1038/Nrm1858**
133. Zervantonakis IK, Hughes-Alford SK, Charest JL, Condeelis JS, Gertler FB, Kamm RD. 2012. Three-dimensional microfluidic model for tumor cell intravasation and endothelial barrier function. *PNAS* 109(34):13515–20. **https://doi.org/10.1073/pnas.1210182109**
134. Hassell BA, Goyal G, Lee E, Sontheimer-Phelps A, Levy O, et al. 2017. Human organ chip models recapitulate orthotopic lung cancer growth, therapeutic responses, and tumor dormancy in vitro. *Cell Rep.* 21(2):508–16. **https://doi.org/10.1016/j.celrep.2017.09.043**
135. Chen MB, Whisler JA, Frose J, Yu C, Shin Y, Kamm RD. 2017. On-chip human microvasculature assay for visualization and quantification of tumor cell extravasation dynamics. *Nat. Protoc.* 12(5):865–80. **https://doi.org/10.1038/nprot.2017.018**
136. Xu H, Li Z, Yu Y, Sizdahkhani S, Ho WS, et al. 2016. A dynamic in vivo–like organotypic blood-brain barrier model to probe metastatic brain tumors. *Sci. Rep.* 6:36670. **https://doi.org/10.1038/srep36670**
137. Chen MB, Lamar JM, Li R, Hynes RO, Kamm RD. 2016. Elucidation of the roles of tumor integrin β1 in the extravasation stage of the metastasis cascade. *Cancer Res.* 76(9):2513–24. **https://doi.org/10.1158/0008-5472.CAN-15-1325**

138. Boussommier-Calleja A, Atiyas Y, Haase K, Headley M, Lewis C, Kamm RD. 2019. The effects of monocytes on tumor cell extravasation in a 3D vascularized microfluidic model. *Biomaterials* 198:180–93. **https://doi.org/10.1016/j.biomaterials.2018.03.005**
139. Sica A, Mantovani A. 2012. Macrophage plasticity and polarization: in vivo veritas. *J. Clin. Investig.* 122(3):787–95. **https://doi.org/10.1172/JCI59643**
140. Ayuso JM, Truttschel R, Gong MM, Humayun M, Virumbrales-Munoz M, et al. 2019. Evaluating natural killer cell cytotoxicity against solid tumors using a microfluidic model. *OncoImmunology* 8(3):1553477. **https://doi.org/10.1080/2162402x.2018.1553477**
141. Wikswo JP, Curtis EL, Eagleton ZE, Evans BC, Kole A, et al. 2013. Scaling and systems biology for integrating multiple organs-on-a-chip. *Lab Chip* 13(18):3496–511. **https://doi.org/10.1039/c3lc50243k**
142. Abaci HE, Shuler ML. 2015. Human-on-a-chip design strategies and principles for physiologically based pharmacokinetics/pharmacodynamics modeling. *Integr. Biol.* 7(4):383–91. **https://doi.org/10.1039/c4ib00292j**
143. Stahl WR. 1965. Organ weights in primates and other mammals. *Science* 150(3699):1039–42. **https://doi.org/10.1126/science.150.3699.1039**
144. Edington CD, Chen WLK, Geishecker E, Kassis T, Soenksen LR, et al. 2018. Interconnected microphysiological systems for quantitative biology and pharmacology studies. *Sci. Rep.* 8(1):4530. **https://doi.org/10.1038/s41598-018-22749-0**
145. Maschmeyer I, Lorenz AK, Schimek K, Hasenberg T, Ramme AP, et al. 2015. A four-organ-chip for interconnected long-term co-culture of human intestine, liver, skin and kidney equivalents. *Lab Chip* 15(12):2688–99. **https://doi.org/10.1039/c5lc00392j**
146. Oleaga C, Bernabini C, Smith AST, Srinivasan B, Jackson M, et al. 2016. Multi-organ toxicity demonstration in a functional human in vitro system composed of four organs. *Sci. Rep.* 6(1):20030. **https://doi.org/10.1038/srep20030**
147. Zhang YS, Aleman J, Shin SR, Kilic T, Kim D, et al. 2017. Multisensor-integrated organs-on-chips platform for automated and continual in situ monitoring of organoid behaviors. *PNAS* 114(12):E2293–302. **https://doi.org/10.1073/pnas.1612906114**
148. Herland A, Maoz BM, Das D, Somayaji MR, Prantil-Baun R, et al. 2020. Quantitative prediction of human pharmacokinetic responses to drugs via fluidically coupled vascularized organ chips. *Nat. Biomed. Eng.* 4(4):421–36. **https://doi.org/10.1038/s41551-019-0498-9**
149. Traore MA, George SC. 2017. Tissue engineering the vascular tree. *Tissue Eng. B* 23(6):505–14. **https://doi.org/10.1089/ten.teb.2017.0010**
150. Mestas J, Hughes CC. 2004. Of mice and not men: differences between mouse and human immunology. *J. Immunol.* 172(5):2731–38. **https://doi.org/10.4049/jimmunol.172.5.2731**

Annual Review of Biomedical Engineering

Volume 23, 2021

Contents

Errata

An online log of corrections to *Annual Review of Biomedical Engineering* articles may be found at http://www.annualreviews.org/errata/bioeng